National Report on Ocean Remote Sensing in Russia

CONTENTS

1. Status of Remote Sensing utilization in marine environmental monitoring

Russian specialists gained multiyear experience in creation and exploitation of space means of remote sensing of the Earth, possess unique scientific-methodological apparatus for remote information processing. Since 1960 operational meteorological space system is successfully in service. The system is based on of "Meteor" series space apparatuses. System of investigation of natural resources based on "Meteor-Priroda" satellites is in service since 1974. "Meteor" and "Meteor-Priroda" satellites used visible and infrared sensors.

Passive microwave sensing of the ocean started in the U.S.S.R. in the early 1960s. The first two satellites to carry four microwave radiometers into space were Kosmos-243 launched in 1968 and Kosmos-384 in 1970; their radiometers operated at wavelengths of 8.5, 3.4, 1.35 and 0.8 cm. The possibilities of retrieving sea surface temperature, near-surface winds, total atmospheric water vapor content, total cloud liquid water content, and sea ice parameters were documented by Basharinov et al. (1974).

The first specialized oceanographic satellites Kosmos-1076 and Kosmos-1151 with microwave radiometers were launched in 1979 and 1980 (Nelepo et al., 1983).

Kosmos-1500, the first satellite to carry a real aperture radar (RAR), was launched in 1983. This RAR operated at a wavelength of 3.15 cm (X-band) with vertical polarization; the swath width was about 460 km, and the spatial resolution was 2.1-2.8 (in flight direction) by 0.8-3 km (normal to flight). A 37-GHz horizontally polarized side-scanning microwave radiometer and four-channel visible imaging system were also carried on Kosmos-1500. This set of sensors was also flown on Kosmos-1602 (launched in 1984) and Kosmos-1776 (in 1986), as well as the Okean series satellites (Kalmykov, 1996).

Results from Kosmos-1500, -1602 and -1776 have been presented Mitnik and Victorov (1990). The unique capability of this series, the simultaneous acquisition of overlapping images by three different sensors at three different wavelengths, enabled an improved interpretation of measurements and a reduction in errors of retrieved parameters. (Such a capability would be employed on later satellites such as TRMM and ADEOS-II). Active and passive sensors, being sensitive to different physical properties of the ocean-atmosphere interface, provide results that complement each other.

The Russian Okean-7 and Okean-8 RAR-equipped satellites were launched in 1994 and 1995, with the last RAR images taken by Okean-7 in February 2000. Satellite RAR images with their 1- to 3-km spatial resolution have been an important source of mesoscale and sub-synoptic scale information on sea ice, near-surface winds for air-sea interaction, and ocean dynamics. Radar images have been used operationally, especially in preparation of maps of ice conditions (Mitnik and Victorov, 1990).

The first U.S.S.R. SAR was carried by Kosmos-1870 launched in 1987, and the second by the space station Almaz-1 (Diamond) in 1991. This SAR operated at a wavelength of 9.6 cm with horizontal polarization; the spatial resolution was 10-15 m within a swath width of 35-55 km. The analysis and interpretation of the SAR images of the sea surface acquired by Almaz-1 SAR are presented by Karlin (1999).

It is clear that passive and active microwave sensing has significant capability for observing oceanic and atmospheric processes. These data have resulted in a series of quantitative scientific findings and theoretical advances in open-ocean, coastal-ocean and marine operations, sea ice, and marine boundary layer meteorology, environmental monitoring including oil spill detection (Mitnik, 2003; Wilson et al., 2006).

Research and monitoring of the ocean and in particular, Far Eastern Seas are carried out in accordance with the Federal Space Program (FSP) of Russia (2001-2005), Statement on State monitoring of environment (State ecological monitoring) and Federal Target-Oriented Program "World Ocean" (2003-2007).

Federal Space Program of Russia (2001-2005) includes Remote Sensing of the Earth, hydrometeorological observations, ecological monitoring and exception situation monitoring.
In particular, the following problems are solved with the using of space technique (http://www.federalspace.ru/fkp_razdel1_2.asp):

- Monitoring of sources of the atmosphere, water and soil pollution to provide information for the state and regional units of environmental control;
- Operational monitoring of natural and technogenic exceptional situations (catastrophes)
- Lunching of space apparatuses "Meteor-M" and "Electro-L" and their using in international system of hydrometeorological observations;
- Performance of experiments with Russian-Ukrainian space apparatus "Sich-1M";
- Receiving, processing and distribution of remote sensing data from Russian and foreigner satellites.

In the frames of the acting Federal Space program (2001-2005), two satellites were launched:

- "Meteor-3M" # 1 for hydrometeorological monitoring in 2001 and
- "Arkon-1" # 2 space apparatus of double purpose for operational and natural resources observations in 2002.

Due to low funding of works on remote sensing of environment conducted in accordance with the Federal Space program as well as due to the system miscalculations and archaic construction decisions an orbital group of Russian RS space apparatuses ceased in fact to operate. Only "Meteor-3M" # 1 performs limited observations (Chernyavskiy, 2004).

In 2003-2004, the following works continued: data processing collected by "Resurs-DK" satellite, experiments with "Meteor-3M" # 1, development of working documents and software for a new generation satellite "Resurs-O1", usage of "Arkon-1" № 2. Additionally, development of all-weather double purpose "Arkon-2" space apparatus (http://www.laspace.ru/rus/arcon.php) and promising hydrometeorological space apparatus "Electro-L" continued.

Federal Space Program of Russia (FSP-2015) on 2006-2015 was approved by Government decree # 635 dated on 22 October 2005. The significant increase of finance of Space sector was suggested and recently approved by the Ministry of Economic Development of Russian Federation.

Statement on State monitoring of environment (State ecological monitoring) was accepted by Government of Russian Federation (Decision from 31.03.2003 # 177). The following points are in the Statement:

- State monitoring of the Environment (ecological monitoring) is the integrated system of observation for the Environment state, for estimation and forecast of its changes under influence of natural and anthropogenic factors;
- Ecological monitoring includes monitoring of atmospheric air, land, forest, water objects, continental shelf of RF, exceptional economical zone of RF, internal sea waters and territorial sea of RF;
- Organization and realization of the Ecological monitoring afford: Ministry of natural resources (coordinator), Federal Serves of RF on Hydrometeorology and Environment Monitoring, State Committee on Fishery and others.

The tasks, which have been formulated in **Federal Target-Oriented Program "World Ocean"** (2003-2007) include:

- Comprehensive investigation of oceanic processes, characteristics and resources of Far Eastern Russian seas.
- Investigation of the state and operation of marine ecosystems of the Far Eastern seas and their productive possibilities.
- Comprehensive study of the state and variability of the coastal zone of the Far Eastern seas

The main goal of the Program is to investigate dynamic phenomena and processes in the Far Eastern Seas and in the Northwestern Pacific Ocean on the basis of development and application of remote acoustic, optical and passive and active microwave techniques.

The project will allow studying the structure, composition and spatial distribution of meso- and submesoscale unhomogeneities, their temporal variability using remote techniques in the Japan and Okhotsk Seas including a shelf zone and transition zone between shallow waters and deep sea.

Systems of operational detection and forecast of transfer and degradation of oil pollution adapted to the Primorye and Sakhalin shelf conditions will be created.

These investigations are currently central and have an additional support in connection with development of the International projects in the Northwestern Pacific such as **NEAR-GOOS, COOP, NOWPAP/UNEP** and **ICZM**.

Participants: *Institutes of Far Eastern Branch of the Russian Academy of Sciences – FEB RAS (POI, IMTP, IACP, PIG, IMB), FIRHRI, Physics and Information Technology Institute of Far Eastern State University, Institute of Oceanology, RAS (Moscow), Pacific Scientific Research Fisheries Centre (TINRO-Centre).*

Table 1. Status of Remote Sensing utilization in marine environmental monitoring

Sensor	Satellite	Variables	Observing cycle	Intended use of data
SAR	ERS-2	Normalized radar cross-section (NRCS) σ^{o}	35 days *)	Coastal and open sea monitoring, detection of oil pollution, natural slicks, oceanic dynamic features, coastal circulation, river plumes, sea ice, near surface wind patterns
ASAR	Envisat	NRCS σ^{o}	35 days *)	Coastal and open sea monitoring, detection of oil pollution, natural slicks, oceanic dynamic features, coastal circulation, river plumes, sea ice, near surface wind patterns
AMSR-E	Aqua	Brightness temperatures at 6 frequencies (12 channels)	14 orbits/ day	Fields of SST, wind speed, precipitable water cloud liquid water content and precipitation in marine weather systems and sea ice
Scattero - meter	QuikSCAT	NRCS σ^{o}	93% of daily coverage	Sea surface wind speed and direction Real-time QuikSCAT data are fully and openly available at <http://manati.wwb.noaa.gov/quikscat/>
Altimeter	ERS-2, Topex/ Poseidon, Envisat, Jason-1, GFO,	Along-track and high-resolution maps of sea level anomalies, along-track and maps of absolute dynamic topography	2 maps/ week	High resolution (1/3°x1/3° on a Mercator grid) maps of sea circulation, eddies' location and intensity Real or near-real time data at: http://www.jason.oceanobs.com/html/
SeaWiFS	OrbView-2	Spectral brightness		Fields of ocean colour (chl *a*), yellow substance absorption coefficient, detection of oceanic dynamic phenomena
MVISR	Feng Yun-1D	Spectral brightness (10 channels)	2-times/ day	Monitoring currents, frontal zones, eddies, upwelling, sea ice as well as the weather systems singly or in combination with other satellites/sensors. Fields of ocean colour (chl *a*), detection of oceanic dynamic phenomena
MODIS MERIS	Terra, Aqua Envisat	Spectral brightness	14 orbits/ day 35 days *)	Fields of ocean colour (chl-a), detection of oceanic dynamic phenomena, sea ice, red tides, cloud patterns

2. Case examples of RS application in marine environmental monitoring

2.1. FEB RAS Centre for Regional Satellite Monitoring of Environment

The FEB RAS Centre for the Regional Satellite Monitoring of Environment is established at 1999 on the base of the *Satellite Monitoring Laboratory of the Institute of Automation and Control Processes, FEB RAS* with participation of the *V.I. Il'ichev Pacific Oceanological Institute, FEB RAS* and *TINRO-Centre.*

The Centre has also International registration as **Satellite Monitoring Laboratory/Institute of Automation and Control Processes/Russian Academy of Sciences (SML/IACP/RAS)** in Global Change Master Directory (GCMD)
http://www.iacp.dvo.ru http://www.satellite.dvo.ru/

The main mission of the Centre is receiving, processing, transferring and archiving of satellite data for monitoring of the ocean and the atmosphere. Now it receives and archives the information from polar NOAA satellites and from geostationary GMS-5 (Japan) and FY-2B (China) satellites.

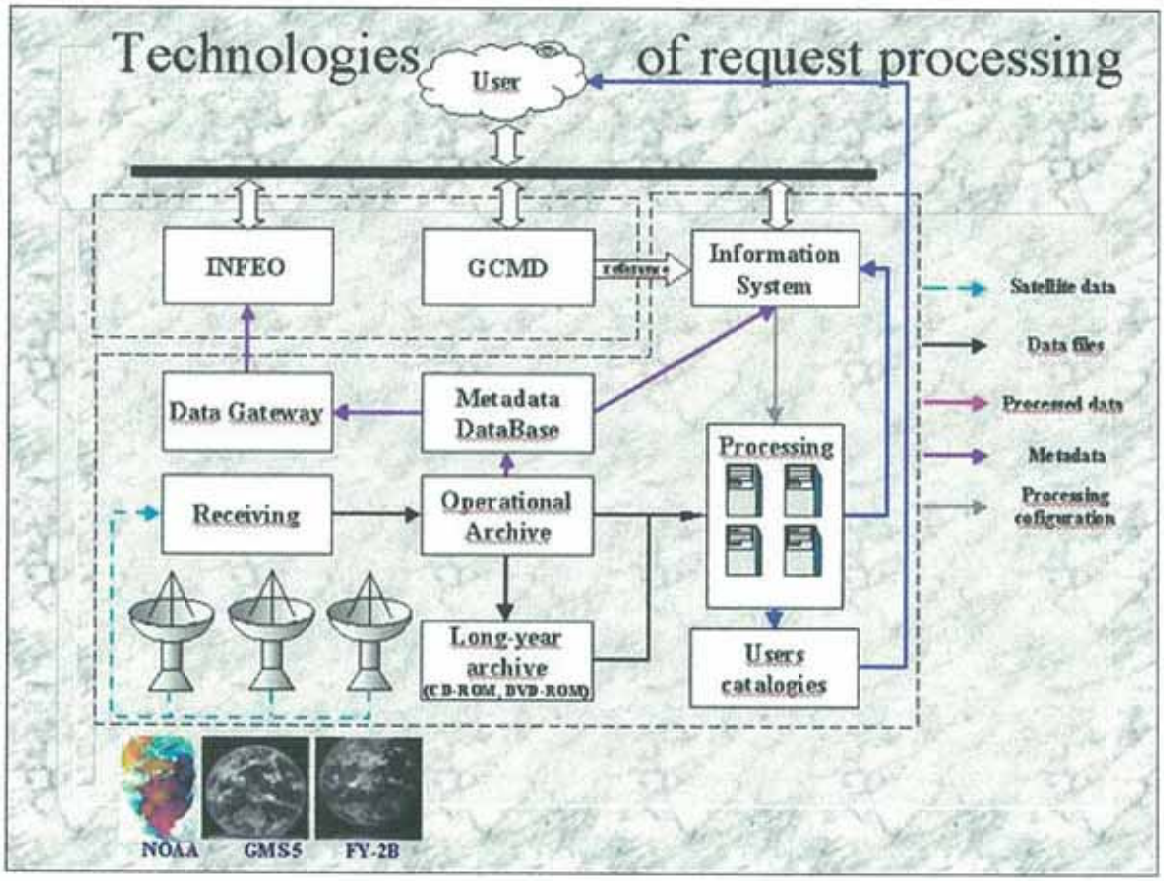

Figure 1. Technologies of request processing at the FEB RAS Centre for Regional Satellite Monitoring of Environment

Output products of the Centre include (Figures 2-6):

- Calibrated images in Mercator projection (pixel size is 1.1 km x 1.1 km);
- SST maps in isolines and in 24- and 48-color temperature scales, retrieved from several individual images with accuracy of 0.5°C;
- Surface current velocities computed with the using of marine marker technique;

- Dominant orientations of thermal contrasts.

All products were tested in operational regime (Aleksanin et al., 2003, 2004a).

The Centre conducts the *Regional Satellite Monitoring* of various objects and processes in the frames of scientific programs and applications of Institutes participated.

Objects of monitoring

- *currently:* Sea surface temperature, frontal zones, eddies, currents, sea ice; typhoons, etc.
- *in prospect:* oil pollution at the sea, floods, forest fires.

Applications of monitoring:

- scientific investigations (physical oceanography and meteorology);
- information support of maritime cruises;
- productivity evaluation and forecast of fishing areas (with TINRO-Centre).

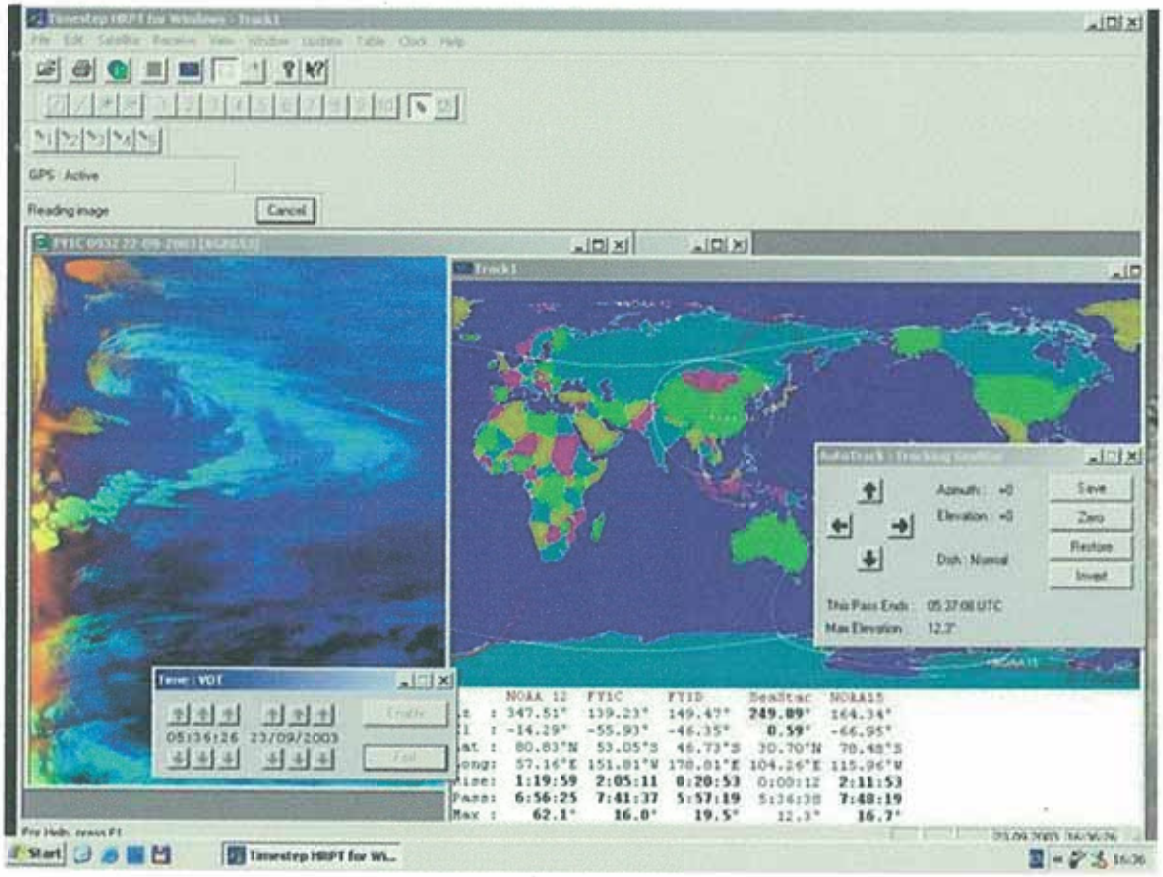

Figure 2. Ground station allows receiving and processing data from NOAA series satellites and from China Feng Yun satellites having additional visible and infrared channels.

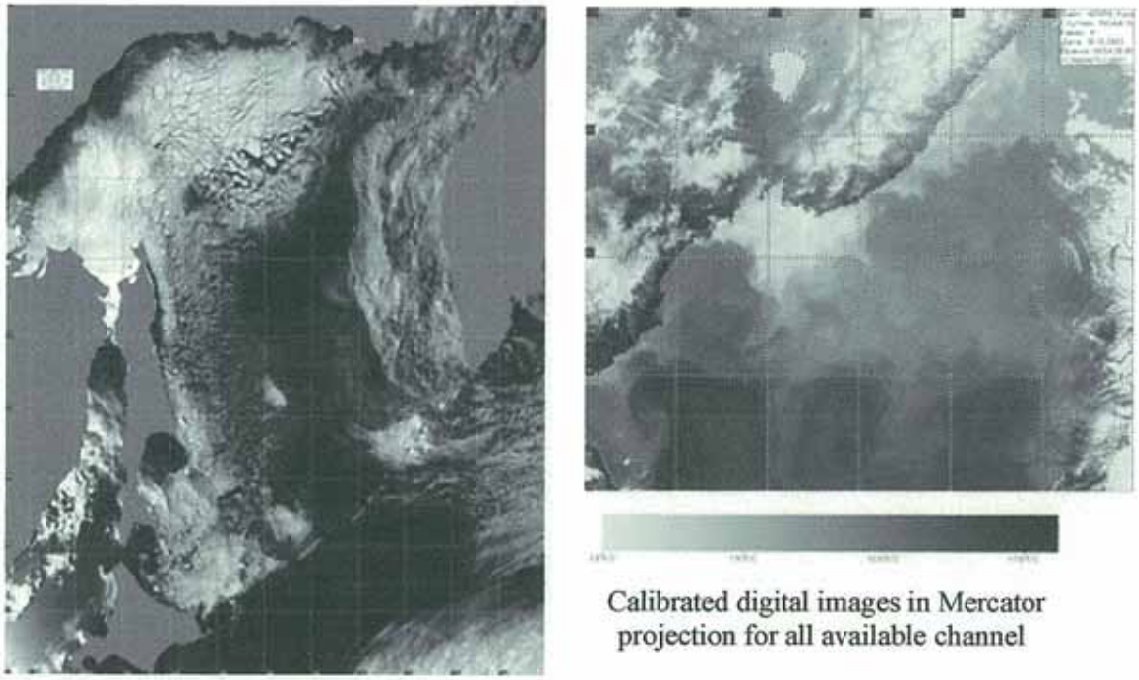

Calibrated digital images in Mercator projection for all available channel

Figure 3. Products of the Centre of Regional Satellite Monitoring

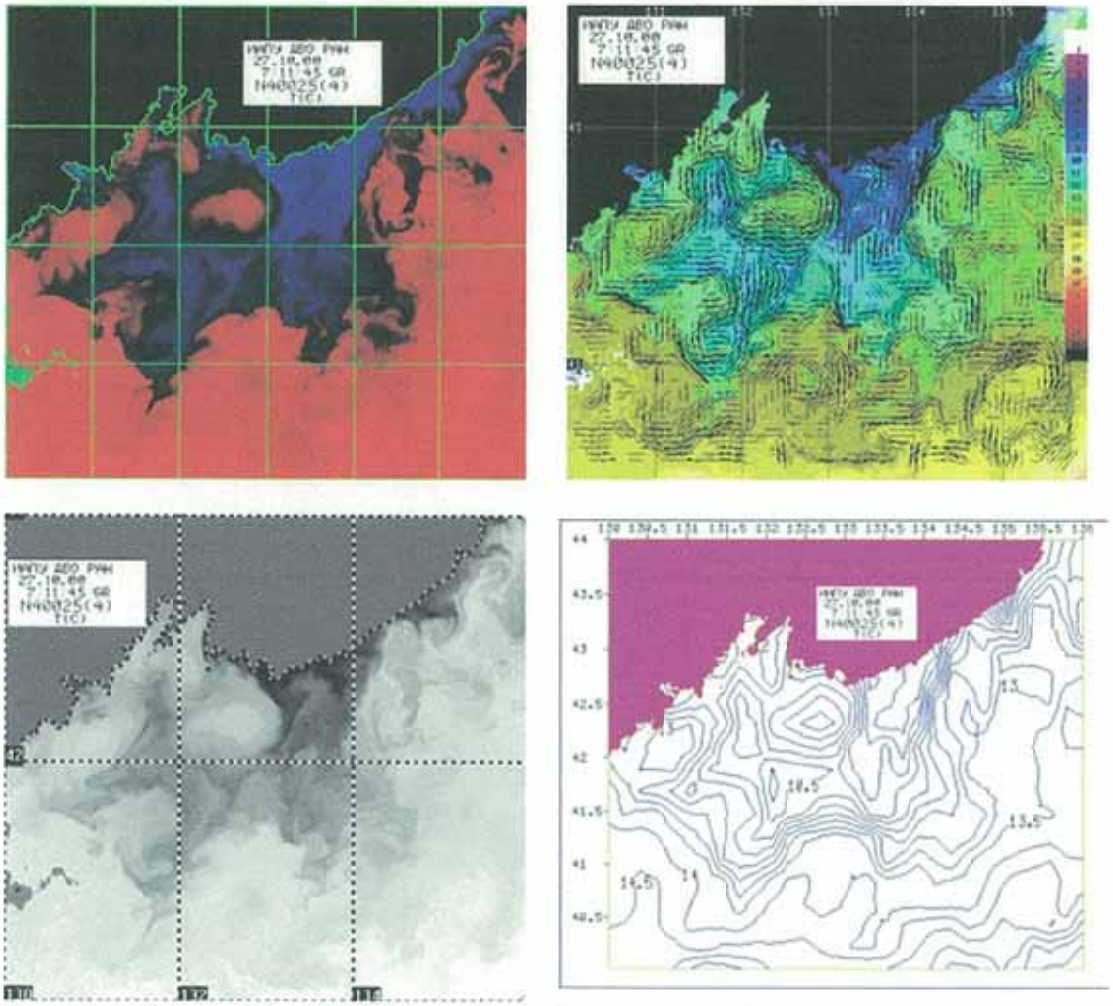

Figure 4. Four versions of SST product for 27 October 2000 to fit users' requirements.

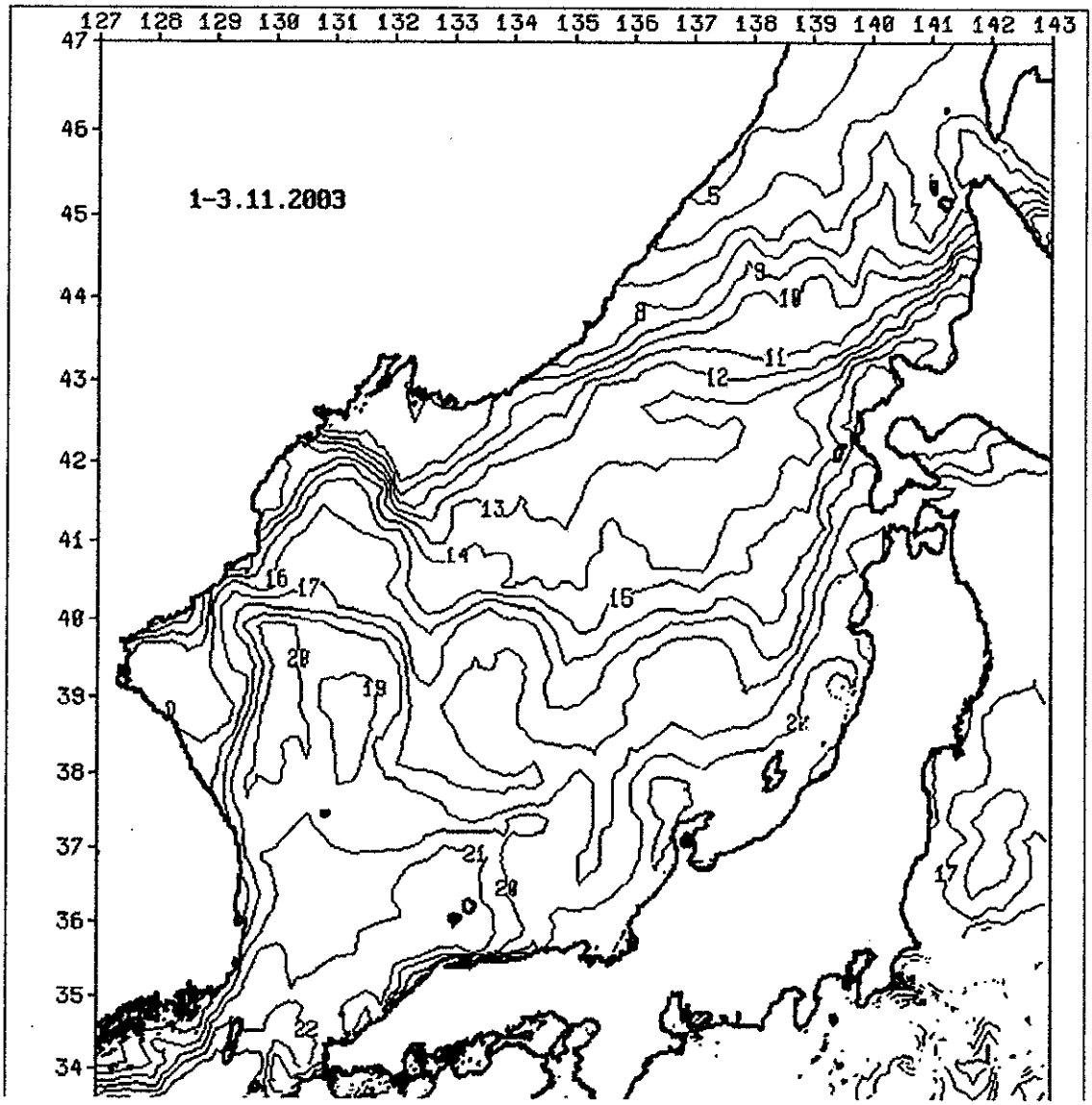

Figure 5. NOAA AVHRR-derived contour SST map

SST maps can be classified in accordance with the scale of spatial-temporal averaging:

(a) maps averaged for 5-10 days with a resolution of 50-100 km;
(b) composition maps with 2-4 days averaging and with a resolution of 10-20 km;
(c) maps constructed from the single NOAA AVHRR image with a resolution of 5 km.

2.1.1 Automatic delineation of vortex structures

The features of oceanic circulation such as fronts, eddies, jets, etc, manifest themselves clearly on satellite IR images. Automatic delineation of these features as well as estimation of their spatial and dynamic parameters is one of the most important problems of the ocean monitoring. High probability of cloudiness, the presence of warm and cold fogs, increased humidity and variable amount of aerosol are typical for Far Eastern Seas. Thus the task is the adaptation of the methods under development to complex environmental conditions.

It was suggested to reveal the thermal structures on the ocean surface using the directed structures Dominant orientation of thermal contrast (DOTC) was used as the main factor. The DOTC properties were investigated and developed software was applied to the NOAA AVHRR thermal images [Alexanin and Alexanina, 2004]. The method allowed to estimate the surface current velocity and the location of eddies' centres (Figure 6).

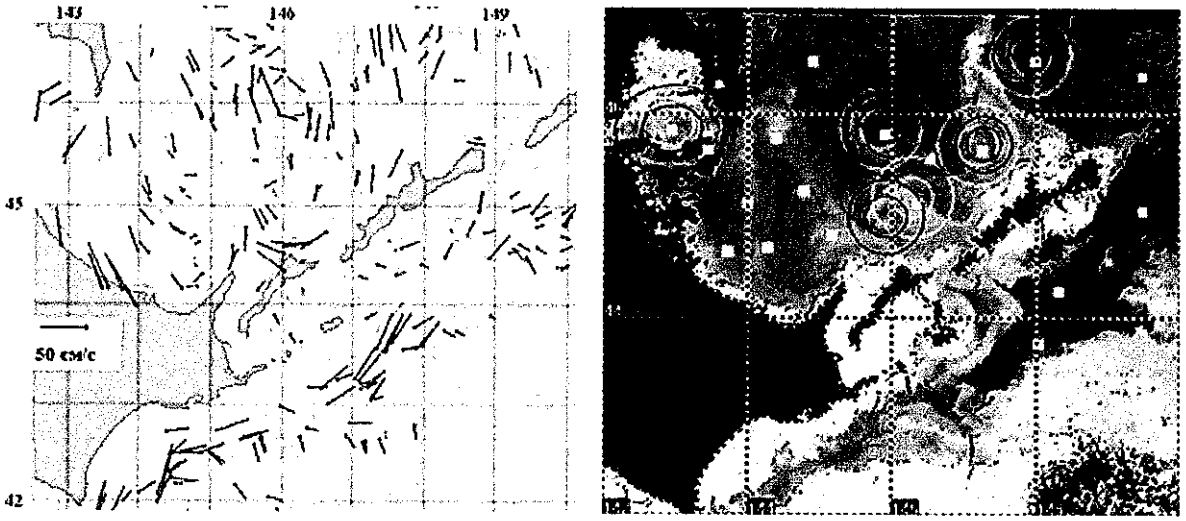

Figure 6. Estimation of surface current velocity and eddies' centres

Surface current velocity (left) and eddies location and boundaries (b). Potential eddies' centres are marked by white rectangles. White ellipses show the first approximation of eddies' boundaries and dark ones – the boundaries after optimization.

2.2. Oil spill monitoring

2.2.1 Detection of oil spills by satellite remote sensing

Satellite instruments are well adapted to monitor and therefore to detect oil pollution since they produce regularly images of the sea surface including the remote areas. Several kinds of measurements have been tested: optical, infrared, radars with different frequencies. SAR seems to be one of the most suitable instruments to the detection of slicks since slicks damp strongly short waves measured by SAR and oil spills appear as a dark patch on the SAR image. SAR observations do not depend on weather (clouds) and sunshine, which allows showing illegal discharges that most frequently appear during night. SAR can also survey storms areas, where accident risks are increased.

The most suitable SAR configuration for oil pollution study is C-band radar frequency with VV polarization, with a 20 to 45° incident angle. This is the case for the European Space Agency (ESA) ERS and Envisat satellites as well as for Canadian RADARSAT. The spatial coverage is adapted to pollution survey: swath width L = 100 km for ERS; 300 km for RADARSAT and 405 km for Envisat Wide Swath ASAR. The pixel size of precision (PRI) images is 12.5 m x 12.5 m for ERS-1 and ERS-2. For Envisat Advanced SAR (ASAR) the pixel size changes from 12.5 m x 12.5 m at L = 100 km to 75 m x 75 m at L = 405 km. ERS-1 operated in 1991-1996. ERS-2 and RADARSAT operate since 1995 and Envisat - since 2002. A problem is the satellite coverage frequency (35 days for ERS-1/2), but now Envisat ASAR allows covering every 3-4 days for accident cases.

A trained human operator is mostly able to discriminate between oil slicks and look-alikes based on experience, visual spill properties (shape and contrast between the feature and the surrounding sea), the presence and location of moving ships, oil platforms and other stationary objects relative to the dark features, etc.). The SAR signature of an oil spill and its surroundings as well as the spill shape depend on a number of parameters like wind speed, wave height, amount and type of oil released. The shape of the spill will also depend on the wind and current history between the release and the image acquisition (Figures 7 and 8).

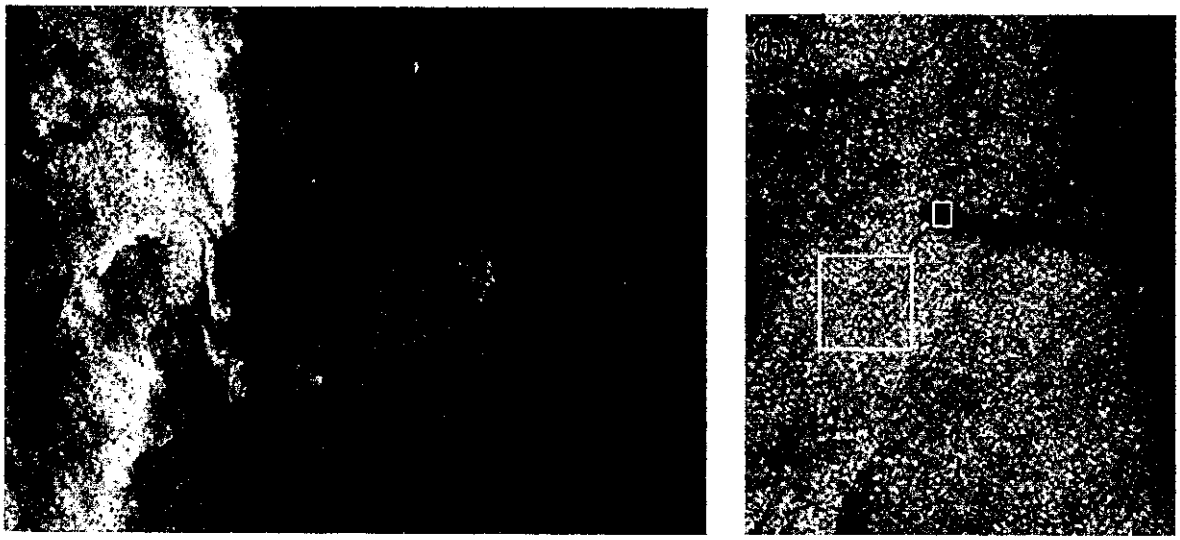

Figure 7. Subsections of ERS-2 SAR images for 20 May 1994 at 14:20 UTC (a) and for 23 March 1999 at 13:27 UTC (b) showing illegal discharge of oil-polluted waters by ships.

Ships are clearly visible as white dots at the beginning of dark bands due to damping of the sea surface roughness by oil. *Fresh discharge* from a moving ship: dark band broadens with the increase of the distance from the ship. The current shift zones (narrow light curvilinear bands)

deform shape of the oil band (a). *Old discharge*: ship is at anchor. Width of the oil spill does not change (b) (CEARAC Website).

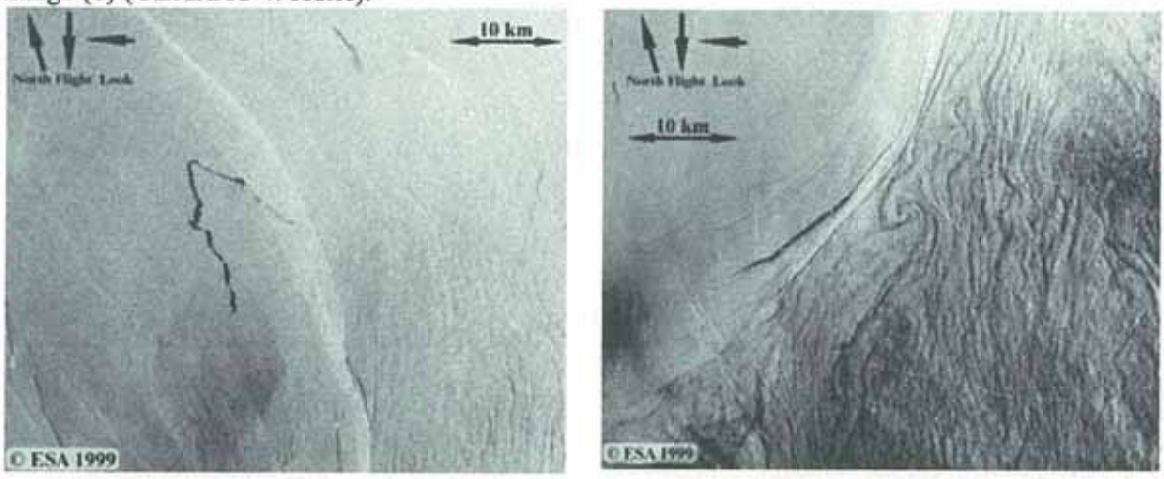

Figure 8. Fragments of ERS-2 SAR image of the Korean Warm Current (KWC) area for 27 September 1999 at 01:30 UTC showing oil spills, natural filamentary slicks, small-scale eddies east of a curvilinear light band (KWC front), ships (bright dots) and ship wakes (Mitnik et al., 2003b).

Several international projects (Clean Sea, DISMAR, Oceanides, etc. –see References in CEARAC Website http://cearac.poi.dvo.ru) and special experiments were arranged to develop effective remote methods and algorithms for oil pollution detection and monitoring. Russian scientists carried out SAR-based study of oil spills in the Black, Baltic and Caspian Seas (Dubina et al., 2003; Ermakov, 2004; Ermakov et al., 2004; Kostyanoy et al., 2004a; Ivanov, 2000; Ivanov et al., 1998, 2002, 2004; Lavrova and Bocharova, 2003; Lavrova et al., 2004; Mityagina et al., 2004). In particular, operational monitoring of oil spills in the southeastern Baltic Sea was organized in June-November 2004 (Lavrova et al., 2004). The following technical means and data sources were used:

- *Envisat ASAR*
  - 3-5 times/week with a resolution of 75 m
  - operational transfer via ftp with a delay less 4 hours
- *NOAA-AVHRR* and *Terra/Aqua-MODIS*
- *QuickScat* – wind speed and direction
- Meteorological information:
  - short time forecast of wind speed and sea surface roughness
  - SST maps
  - showers and heavy clouds (coastal radar)
  - reports of coastal meteorological stations

  Numerical interactive model of currents in the Baltic Sea.

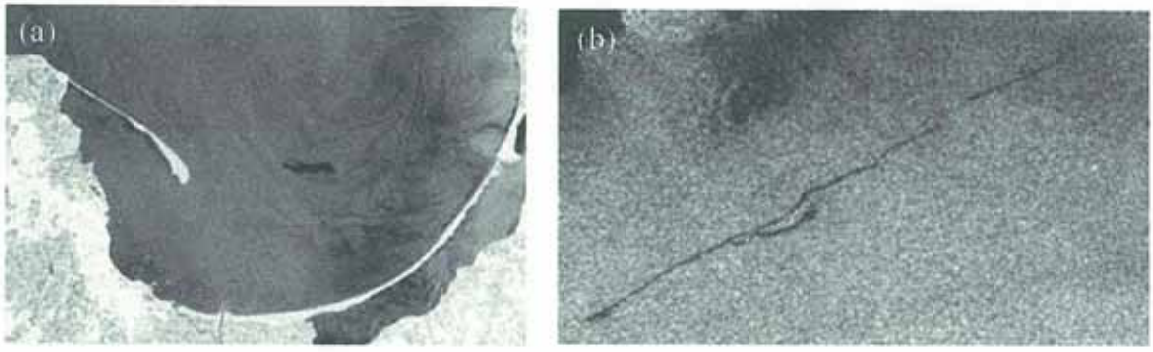

Figure 9. Fragments of Envisat ASAR images of the Baltic Sea taken on 11 August (a) and 2 November 2004 (b).

The area of oil spill in Gdansky Zaliv is about 23 km^2 (a). Oil pollution from a moving ship to the south of Eland Island has a length of about 60 km (b) (Lavrova et al., 2004).

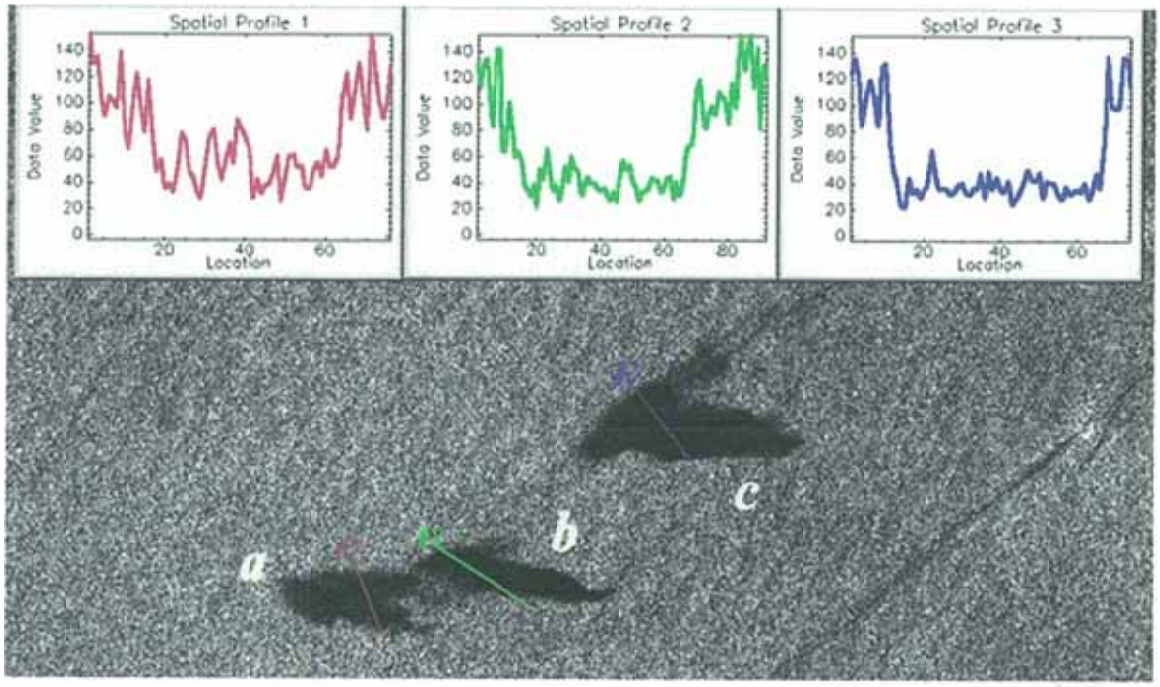

Figure 10. Fragment of ERS-2 SAR image of the Black Sea near the Novorossisk - Gelendjik coast taken on 31 July 2002. *a*, *b* and *c* are oil spills of different age.

Three large dark patches stand out brightly against the background waters due to smoothing of the sea surface roughness caused by three oil discharges *a*, *b* and *c* happened with some delay relative to each other. The sections through the patches are shown in a top of the image. Patch *a* is characterized by the minimum contrast (it appeared earlier) and patch *c* – by the maximum contrast (oil discharge took place later) (Lavrova et al., 2004).

2.2.2 Oil spills study in the NOWPAP region

The SAR images taken over the NOWPAP area are in an archive of the ESA as well as in catalogues of several ground stations located in Japan, China and Taiwan. Only a part of the acquired images was processed. They are available in a form of so named Quick Look (QL) images and can be downloaded from the archives. SAR QL images have the reduced spatial and radiometric resolution. Thus only relatively large scale spills having high radar contrast can be revealed on the QL images.

High-resolution SAR data allow to detect the small-scale spills as well as the oceanic dynamic phenomena (currents boundaries, fronts, eddies, etc.) the location and intensity of which should be taken into account at interpretation of the SAR signatures. SAR PRI images can be ordered at the ESA for payment. For the selected research projects the ESA provide the SAR PRI data free of charge within predetermined quota.

Currently POI carries out research on three ongoing ESA projects dealing with the oceanic dynamic phenomena study in the NOWPAP area: AO3-401 "Mesoscale oceanic and atmospheric phenomena in the coastal area of the Japan and Okhotsk seas: Study with ERS SAR and research vessels", AO3-1291 "Soya Warm Current study with Quick look and Precision ERS SAR images" and Envisat project AO-ID-391 "Study of the interaction of oceanic and atmospheric processes in the Japan Sea and the Southern Okhotsk Sea". Additionally a new international project AOBE.2775 "Detection and parameter estimation of organic pollution in the coastal zone" associated with oil pollution study in the Northern, Baltic and Black Seas and in the NOWPAP area with the usage of satellite SAR images started in 2004. (Participants of this project are Universities and research Institutes in England, Germany, Portugal and Russia). Each SAR image obtained in the frames of these four projects is used in particular for detection of oil spill.

Automatic analysis of SAR images is not applied routinely yet. It is caused by the influence of both technical and natural factors. The contrast between a spill and the surrounding waters, and thus the probability of detecting pollution slicks, depends on the amount and type of spilt oil as well as on environmental factors such as wind speed (it has to be between 2-3 to 10-12 m/s), wave height, SST, currents and current shift zones. Then, it is rather hard to distinguish oil spills from other phenomena which analogously to oil spills have negative radar contrast (look dark on SAR images) relative the surrounding waters and commonly referred to as "look-alikes". Among such "look-alikes", are films of surface active substances (mainly, natural caused by the increased plankton (chlorophyll *a*) concentration) observable frequently at $W < 5$-6 m/s, wind shadow areas near the coast, heavy rains damping small scale roughness, upwelling zones and grease ice.

Several algorithms based on application of different approaches were suggested, realized and tested (Frate et al, 2000; Pavlakis et al., 2001; Lichtenegger, 1994; Lichtenegger et al, 2000; Solberg et al., 1999, 2003, 2004). One of the promising techniques for automatic discrimination of the oil spills is *the calculation of fractal dimension*. Using of the simple box-counting algorithm for SAR image analyzing shows differences in the maximum fractal (box counting) dimension of oil spills compared to other types of oceanic phenomena (Gade and Alpers, 1999; Darkin et al, 2004). Next approach taking to the discrimination (and simultaneously to oil's contour receiving) is *neural networks*. Neural network is leaned on the base of confirmed oil slicks and neurons of the input layer of the network are such features as: texture characteristics, contrast ratio, border gradient and so on (Frate et al., 2000). The algorithms for slick detection and classification based on fractal dimension and neural networks are now tested at POI using ERS-1/2 SAR and Envisat ASAR images of the NOWPAP area.

At present Russia have no possibility to arrange real remote sensing monitoring of oil spills in the NOWPAP area since the receiving stations in Khabarovsk and in Vladivostok have no equipment for SAR data acquisition. All ERS-1/2 SAR and Envisat ASAR PRI images were provided by the ESA for the above mentioned projects. The images (now POI has >350SAR and ASAR PRI images) were ordered after screening the archive QL images or by sending an order to the ESA in advance (2 weeks and more) to collect satellite data during ship or coastal ex periments. More images should be studied to get more reliable statistical estimates, to reveal regional features, to test and tune the developed algorithms for oil spill detection.
Most of the SAR images cover the NOWPAP region. The results of their analysis were presented at International Symposia and published as well as used in CEARAC Website on oil spill.

2.2.3 Website content

The results of preliminary POI research on oil spill detection and monitoring are summarized in the CEARAC Website (http://cearac.poi.dvo.ru). The following sections are in the website (Figure 11):

1 Introduction
2 Behaviour of oil at sea
3 Remote sensing techniques of oil pollution detection
4 Marine satellite remote sensing data used for oil spills monitoring
5 Algorithms of interactive and automatic detection of oil spills
6 Database of the georeferenced satellite SAR images of the Northwest Pacific.
7 References.
8 Links.

Database consists now of several tens of ERS-1 and ERS-2 SAR images (Figure 12). Number of SAR images is supposed to increase and provide annotation for each image.
Links include in particular several sections important for operational usage such as

News (global and regional, tanker incidence, description, pictures, hot satellite images, evolution, role of remote sensing, etc.).

Oil pollution spreading models.

Environmental information important for oil pollution monitoring/evolution (winds, currents, ice, weather forecast) - Links to the China, Japan, Korea, and Russia sources of data.

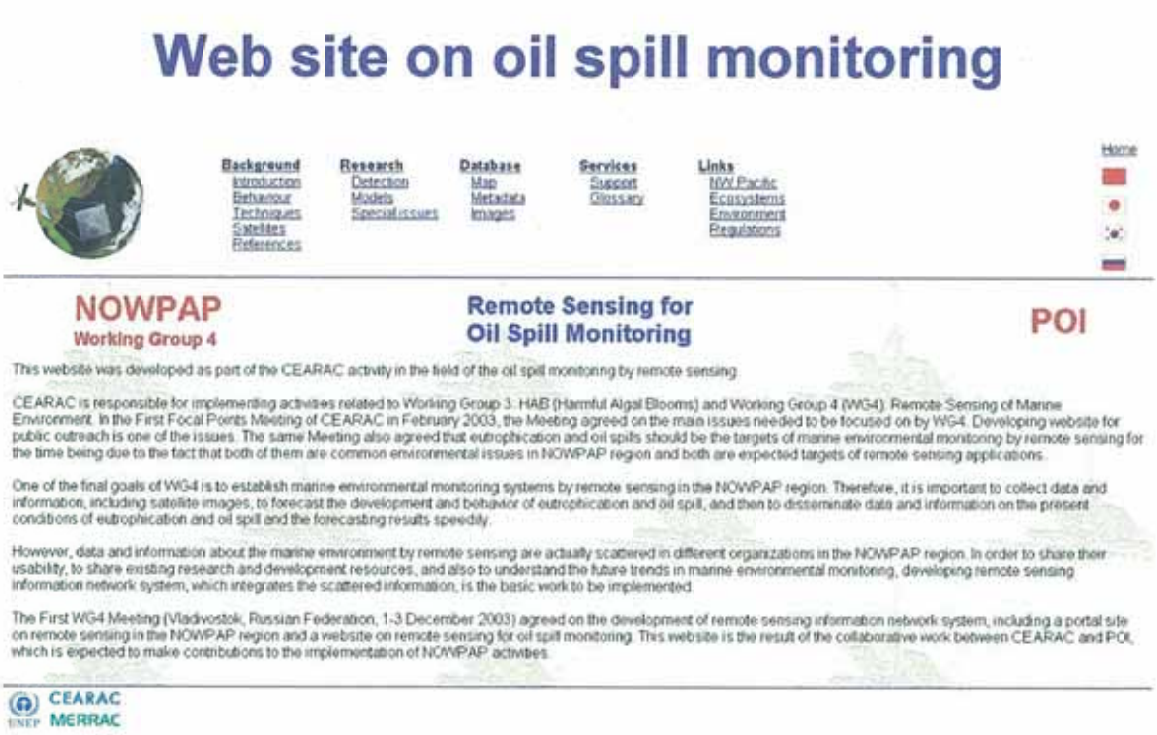

Figura 11. The first page of website http://cearac.poi.dvo.ru

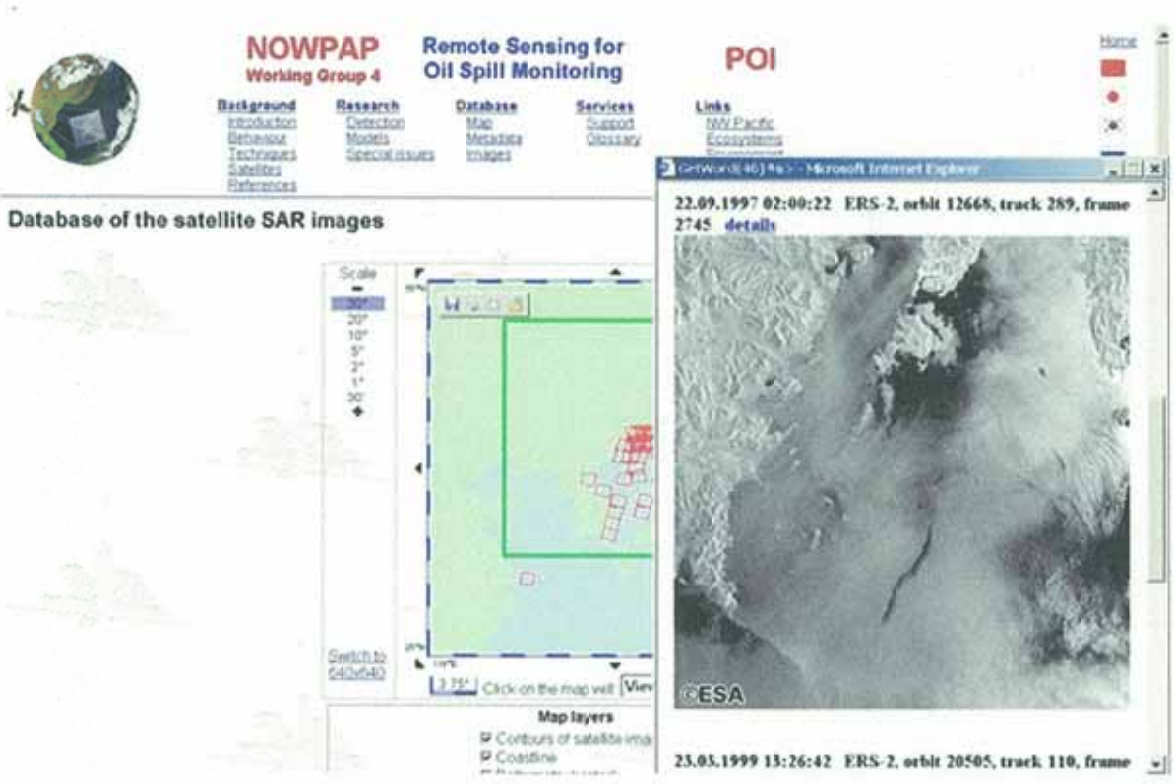

Figure 12. ERS-2 SAR image showing oil pollution in Peter the Great Bay

2.3 The NOWPAP region monitoring using multisensor data

Satellite-based study and monitoring of the NOWPAP region is carried out by several organizations to solve both scientific and applied problems such as weather forecast, marine transportation, fishing, etc. Satellite data serves for retrieval of the various geophysical parameters such as fields of SST, Chl *a* concentration, sea surface height, wind speed and direction, wave height, ice conditions, etc. The most fruitful approach is the joint usage and analysis of the various satellite products.

This approach was realized in All-Russia scientific-research and planning-construction Institute for Economy, Information and Automatic Systems of Management where information technology of remote determination of primary productivity in the ocean was developed (Fefilov, 2003). Data from NOAA, TOPEX/Poseidon, SeaWiFS and ERS-2 as well as information on catch are used in the system to produce a new product by integration of various data. In Figure 13 chl *a* concentration is shown by different colors, sea surface height - by the dark lines and catches - by the circles diameter of which is proportional to catch volume.

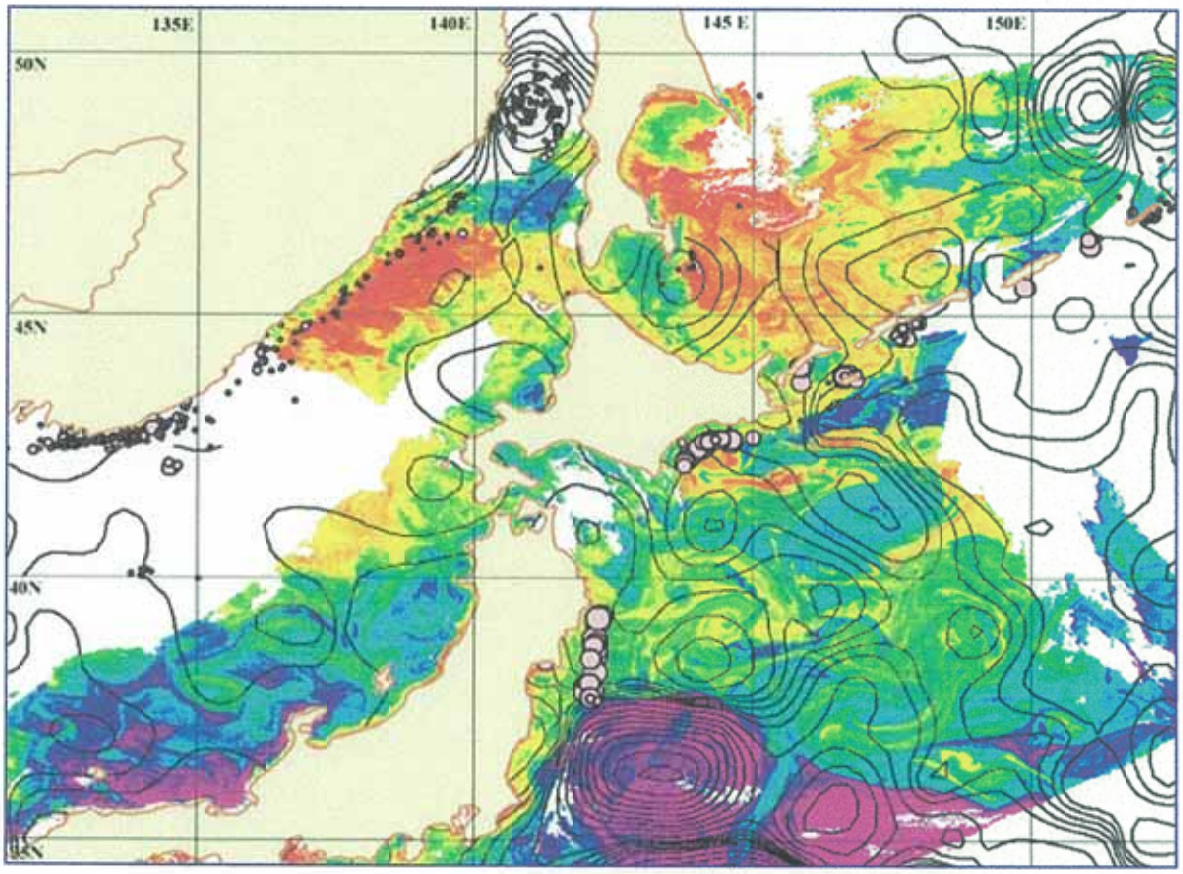

Figure 13. Integration of satellite products with fishing boat catch.

Observations from Russian high- and low-resolution optical satellites (Resurs and Meteor), radar satellites (Okean) and from USA satellites (NOAA, Terra and Aqua) as well as the geographical maps, *in situ* data and other supplementary information were integrated to arrange space monitoring and long-term study of ice cover of the Arctic, White Sea, Caspian Sea, Okhotsk Sea and the NOWPAP region (Trenina, 2004).

Usage of high-resolution data first of all provided by the satellite Synthetic Aperture Radars (SAR) opened the new possibilities for monitoring of the mesoscale and fine scale features of oceanic dynamic phenomena especially when SAR images were analyzed together with other satellite and *in situ* observations.

The imprints of oceanic dynamics were found on about 80% of all SAR images. The following features were revealed:

- *eddies of different scales and chains of eddies,*
- *fronts,*
- currents,
- *internal waves,*
- *upwelling,*
- *river plumes.*

The visual identification of oceanic dynamic phenomena in the NOWPAP area was guided by numerous assessments of **SAR** signatures. Interpretation of radar signatures was confirmed by their comparison with the NOAA **AVHRR** visible and IR images, weather maps, bathymetric maps as well as with the hydrographic observations carried out by POI research vessels. The **AVHRR** data generally supported and enhanced interpretation of **SAR** signatures. Under clear sky, joint analysis of **SAR** and **ocean color** images helped to identify the physical and biological processes controlling the main backscatter features found on the SAR images. **QuikSCAT** measurements and **surface weather maps** provided data on the surface wind speed and direction and sea state close in time to **SAR** sensing. A direct comparison between **SAR** and **altimeter** data was difficult because the temporal and spatial coverage and resolution of the two systems are quite different. The **altimeter** may not capture many of short-lived mesoscale features observed by **SAR**.

The NOAA images were provided by the FEB RAS Centre for the Regional Satellite Monitoring of Environment and by the Far Eastern Regional Centre for Receiving and Processing Satellite Data (Khabarovsk, Russia). Other satellite and supplementary information was downloaded from Internet (see Table 1).

Case studies presented below show the unique capacity of a SAR to detect a variety of the small-scale oceanic features and feasibility of multisensor approach in the ocean phenomena study.

2.3.1 Korean coastal waters

The circulation of this part of the NOWPAP region is characterized by significant temporal and spatial variability due to such factors as seasonal fluctuations in the warm inflow through Tsushima Strait, branching of the Tsushima Warm Current (TWC), and the formation of mesoscale eddies along these branches. Thermal contrasts are usually associated with the warm and cold currents, eddies and upwelling. Although the main features of the circulation are reasonably well known, a detailed description of even dominant currents like the Tsushima Warm Current, East Korean Warm Current, Liman Current etc. still attract oceanographers due to their constantly changing nature. This is especially true for the features of smaller scales.

Consider at first SAR images of the East Korean Bay (Mitnik et al., 2003b). The oceanic processes here have not been adequately investigated in particular due to difficulties in hydrological data acquisition. An anticyclonic eddy at about 39-40°N, 129-130°E exists most of the time (Shin et al., 2000; Suh et al., 1998). The SAR image (Figure 14a) shows this eddy at the end of September when its thermal contrast against the surrounding waters (Figure 14b) is less than in winter. TOPEX/Poseidon data confirms anticyclonic circulation in this area (Figure 14b).

Figure 15a shows plentiful filamentary slicks in the western part of the East Korean Bay resulted very likely from the increased plankton concentration. Their shape suggests that anticyclonic circulation and a possible convergence towards the eddy center were observed. The increased productivity of the eddy area is confirmed by the presence here of intensive fishery: a lot of ships and ship wakes are clearly visible within a small area (Figure 15b) marked by a white rectangle in Figure 15a.

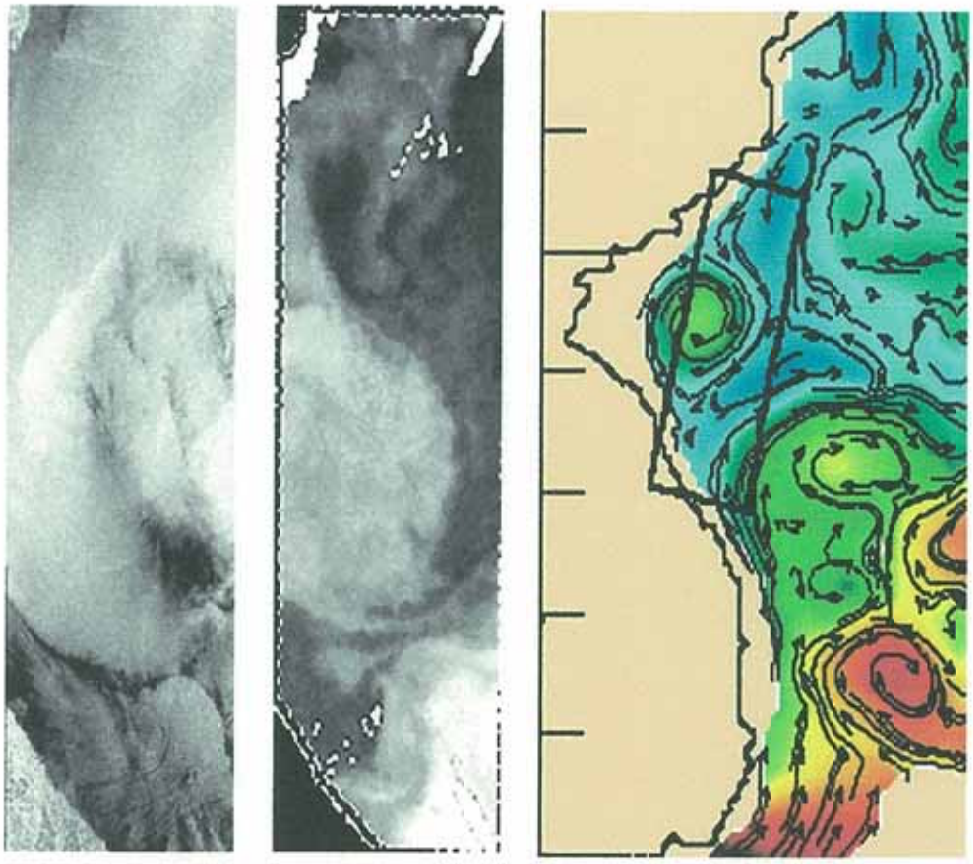

Figure 14. An anticyclonic eddy in the East Korean Bay. (a) SAR image for 25 September 1997 at 02:06 UTC, (b) AVHRR-derived SST for 23 September 1997 at 21:53 UTC and (c) sea surface height (shown by color) and currents (arrows) retrieved from altimeter measurements (http://www7320.nrlssc.navy.mil/global_nlom/globalnlom/soj.html)

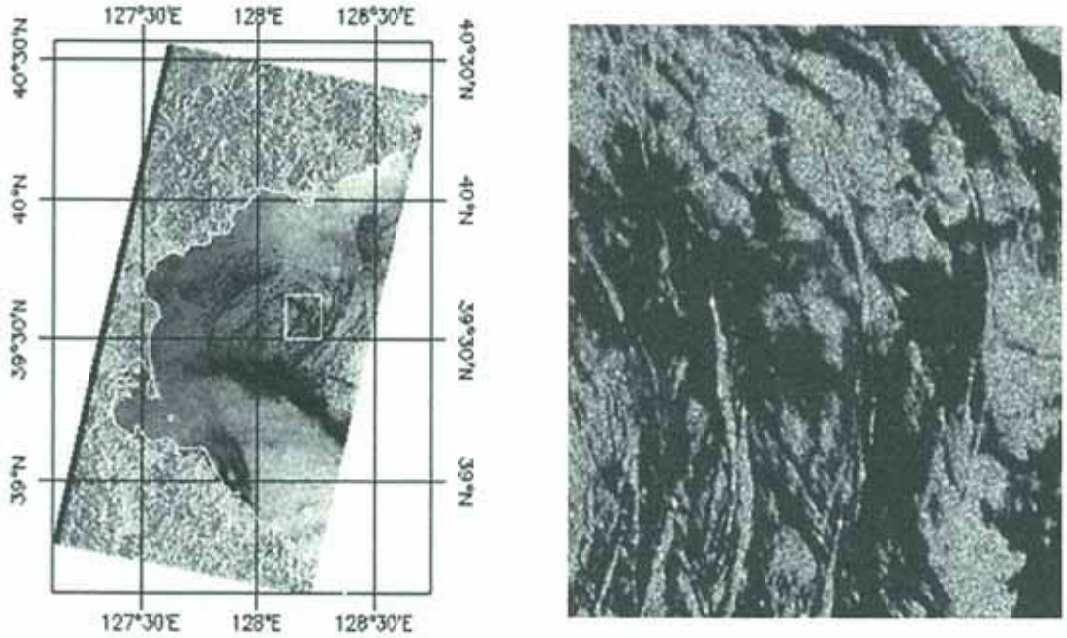

Figure 15. ERS-2 SAR image for 18 August 2002 at 02:11 UTC showing an eddy in the East Korean Bay (a). White rectangle marks the boundaries of a fragment (b) where ships (bright dots) and ship wakes behind them are well defined.

There are few direct observations of internal waves (IWs) east of the Korea coast. As follows from the analysis of the ERS SAR images, significant internal wave activity is observed in the coastal waters due to the combination of high tidal range and the complicated bottom topography. Figure 16 shows one of the many examples of SAR images where there are expressed several IW packets. They appear to propagate in at least three different directions. Some of these IW packets are oriented approximately parallel to the depth contours (blue lines) that run more or less parallel to the Korea coastline. Two packets of nonlinear internal solitary waves propagate northwestward. The packets contain waves with about 10 rank-ordered solitons with monotonically decreasing distance between them (from about 4 km to about 0.5 km). Some interaction among packets propagating in different directions is observed (Mitnik et al., 2003b).

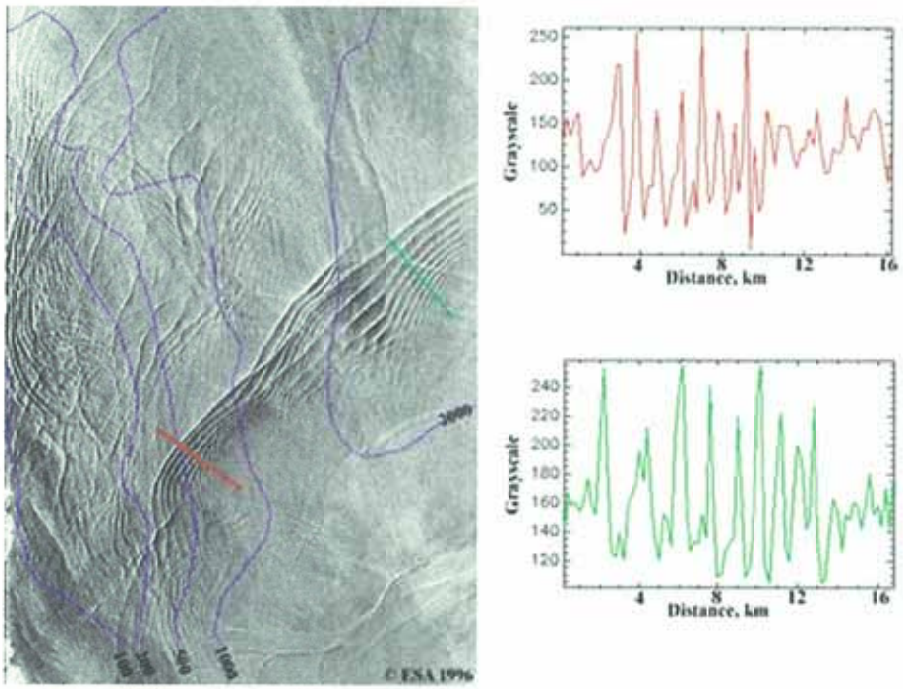

Figure 16. Packets of solitary internal waves on ERS-2 SAR image acquired on 2 September 1996 at 02:02 UTC (a) and sections through two packets showing the decrease in wavelength from front of the packet to its rear (b) and (c).

2.3.2 West Sakhalin Current and Soya Warm Current

The processes in the northern part of the sea (to the north from 46°N) play an important role in the circulation of the sea as a whole. The northernmost area called the Tartar (Tatarski) Strait is connected with the Okhotsk Sea through Nevelskoy Strait. Circulation in this region is mostly wind forced, but, additionally has two stable oceanic components. These are the southward Liman (Shrenka) Current along the western Tartar Strait coast and the West Sakhalin Current (WSC) near the southwestern Sakhalin coast. The WSC represents a narrow band the width of about 15-20 km. This along shore flow carries the cold waters into the Okhotsk Sea through the Soya Strait. Non-tidal current speed of the WSC is about 0.5 m/s, but total current velocity may reach 2.2 m/s in the Soya Strait. The strong current gradients were sometimes observed in the Soya Strait area and on the shelf and slope of the southwestern Sakhalin. The spatial and temporal peculiarities of the current system are poorly known because of little amount of ship hydrological observations and the high probability of cloudiness that hinders regular satellite IR observations.

The main features of the SST field are the cold waters **1** to the west of Krilion Cape, Soya Warm Current **2** along the Hokkaido coast and a narrow belt of cold water **3** adjacent to the current (Figure 17b). The cold waters are traced from Cape Krilion and form a cold belt parallel to the SWC (Danchenkov et al., 1999 and references cited in their paper). The SST field shows the sharp boundaries between waters with the different properties and also reveals the dynamic features such as the current shift zones, eddies, etc. The shape and sharpness of the front between the warm Soya and cold offshore waters as well as wave production after the flow separates from Cape Krilion are likely determined by the current velocity in the Soya Strait, which, in turn, depends on the water level difference between the NOWPAR region and Okhotsk Sea (Ohshima and Wakatsuchi, 1990).

The Soya Warm Current front, a cold belt adjoining to the current from the north and synoptic-scale eddies propagating southeastward parallel to Hokkaido coast as well as spiral eddies in the Aniva Bay were found on many SAR images and studied in details (Dubina and Mitnik, 2004; Mitnik and Dubina, 2003; Mitnik et al., 2004a,b). The boundaries of warm waters flowing into the Okhotsk Sea through the LaPerouse Strait and cold waters around Cape Krilion are clearly visible both on ERS-2 SAR images (Figure 17a,c) and on AVHRR IR image (Figure 17b) taken in ~15.5 h after radar sensing on 14 September (Figure 17a).

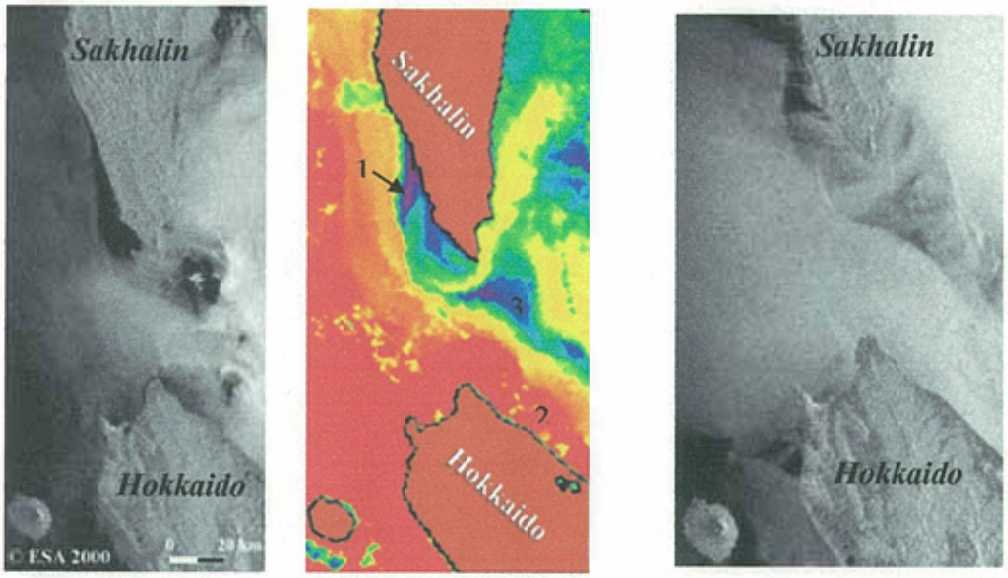

Figure 17. Soya Warm Current and cold waters around Cape Krilion on ERS-2 SAR QL image (a) and on NOAA AVHRR IR image (b) for 14 September 2002 at 01:20 UTC (a) and at 16:50 UTC (b) and on ERS-2 SAR QL image for 5 August 2000 at 01:20 UTC during strong westward tidal current (c).

Collocated ERS-2 SAR and Envisat ASAR images acquired on 4 October 2003 with time difference of about 28 min have trapped the West Sakhalin Current (WSC) during its maximum intensity. The current was observed as a narrow strip the width of about 15 km adjacent to the northwestern Sakhalin coast. Backscatter contrasts in the convergence region between the Tsushima Current and the WSC reached 20 dB. Such contrasts were due to the combined effect of the sea surface temperature difference and wave-current interaction in the convergence and shear zones. The surface manifestations of the several packets of internal waves were clearly visible in the southeastern part of the Tartar Strait and in LaPerouse (Soya) Strait. Transformation of the internal wave packets is noted near the WSC's boundary (Dubina and Mitnik, 2004).

Joint analysis of ERS-2 and Envisat images allowed estimating the movement velocity of the SAR signatures caused by both the oceanic (currents, internal waves, etc.) and atmospheric dynamic phenomena on the southern Sakhalin shelf. The signatures are characterized by the appearance of

both positive and negative contrasts against the background. The tidal outflow moves radar signature **C** to the Hokkaido coast at the speed of 0.4 m/s. At the same time, radar signature **T** moves westward at the speed of 0.7-0.9 m/s (Figure 18). Close inspection of the derived movement shows that the bright radar signature **W** corresponding to the convergence zone between Tsushima Current and West Sakhalin Currents undergoes cyclonic displacement. Its southern part moves to the northwest with the speed of 0.5 m/s and northern part moves coastward with the speed of 0.3 m/s (Figure 18).

A narrow light-dark band in the low right-hand section of Figure 18 is very likely the internal wave soliton. Its northern side moves westward at a rate of 0.8 m/s and the southern one displaces slower (0.3 m/s) due to the Soya Warm Current influence. Several packets of internal waves are visible to the east from the considered soliton. The presence of internal waves confirms that the water stratification and current velocities were favourable for their generation.

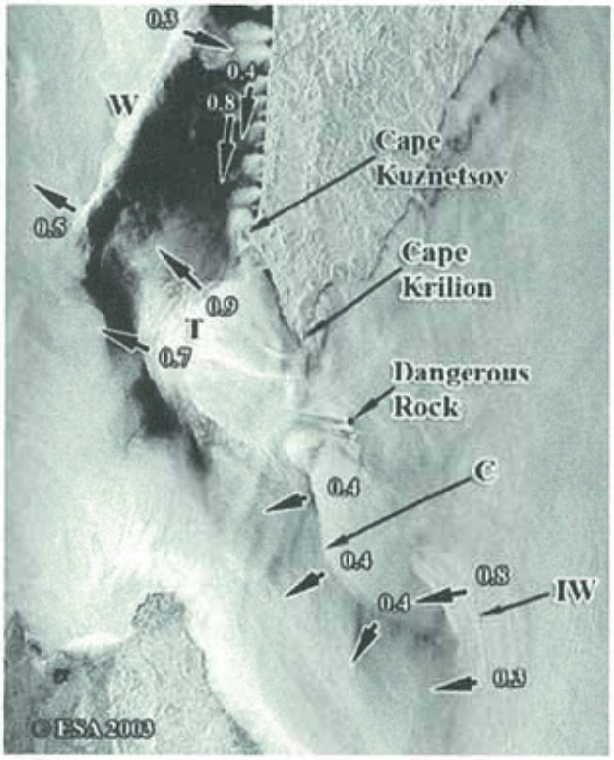

Figure 18. Fragment of the ERS-2 SAR image acquired on 4 October 2003 at 12:41 UTC. Arrows point movement directions and numbers denote movement speeds (m/s) of the radar signatures estimated with the use of the collocated Envisat and ERS-2 images (Dubina and Mitnik, 2004).

2.4 Sakhalin Scientific Research Fisheries Centre (SAKHNIRO-Centre)

http://www.SAKHNIRO.ru

This Center has a TeraScan receiving station to get and analyze information on ocean color in the Okhotsk Sea and in the NOWPAP area. The following Department/Laboratories/Groups participate in research:

- **Group of Network and Information Ensuring**
  http://www.sakhniro.ru/group_of_network_and_information_ensuring.html
- **Department of Applied Ecology**
  Laboratory of Analytical Researches

Laboratory of Applied Ecology
aboratory of Inland Bio resources

- **Laboratory of Coastal Researches**

http://www.sakhniro.ru/laboratory_of_coastal_researches.html

2.5 Marine Oceanography and Marine Environment of the Far Eastern Region of Russia

http://www.pacificinfo.ru/en/

This POI specialized web-site in the FEB RAS Network is an independent regional segment for the National Unified System of Information on the World Ocean State "ESIMO". Information about the data bases maintained at the POI, in the region and over the world as well as about other resources accessible in the on/off-line mode and also information products on various aspects of oceanography, hydrometeorology and ecology are available on this site.

- National and International Regional Projects:

ESIMO, PICES, WESTPAC, NEAR-GOOS (Regional Data Bases), NOWPAP Oceanographic Data Center, other Institutes and Projects

- Marine Research Institutes of Vladivostok
- RIHMI-WDC(B)
- FEB RAS Base Network
-

Catalogues, Data Sets and Data Bases

- *List of Oceanographic Data held by POI*
- *Data Base of POI Oceanographic cruises Data*
- *Integrated Data Base of historical observations*
- *Satellite Data*
- *Geological and Geophysical Data*
- *NEAR-GOOS/POI Data Base*

Project Leader: Igor Rostov, POI FEB RAS rostov@pacificinfo.ru

3. STATUS OF RESEARCH AND DEVELOPMENT ON REMOTE SENSING TECHNOLOGY FOR MARINE ENVIRONMENT

3.1. Sensors and Satellites

3.1.1 Meteor-3M # 2

Satellite Meteor-3M # 2 is planned to launch in 2006. Observations of the ocean will be carried out with the usage of several sensors such as MTVZA-OK (see Table 2), MSU-EU and MSU-S, MIVZA and MTVZA operating in visible, infrared and microwave ranges. Their characteristics are given in Tables 3-5.

Figure 19. Space apparatus "Meteor-3M"

Table 2. Visible, infrared and passive microwave sensors

MTVZA-OK Visible-Microwave Scanner	KM – 4VD (4 channels), μm	0.37-0.78
	KC-IK (1 channel), μm	3.55-3. 93
	KM -2IK (2 channels), μm	10.4-12.6
	Microwave radiometer (11 channels), range, GHz	6.9-183.3
	Swath width, km	2000
	Resolution, microwave radiometer, km x km KM–4VD, KC-IK, KM-2IK, km x km	From 112 x 260 to 8 x19 1.1 x 1.1

Table 3. Visible and near infrared sensors

MSU-EU Optoelectronic Multiband Scanning Device	Spectral ranges, μm	0.5-0.6, 0.6-0.7, 0.8-0.9
	Coverage area width, km	800
	Swath width, km	76 (nadir) / 116(edge)
	Resolution, m x m	32 x 32
MSU-S Medium Resolution Multiband Scanning Device	Spectral ranges, μm	0.55-0.7, 0.7-0.9
	Swath width, km	2240
	Resolution, range / azimuth, m	544 / 142

Table 4. Scanning microwave sensor MIVZA

Microwave scanning radiometer for atmospheric integrating humidity sounding (MIVZA).	20 (V,H)	110	1700 (conic scanning)
	35 (V,H)	65	
	94 (H)	25	

Table 5. Microwave scanning radiometer MTVZA

Parameters	MTVZA								
Frequency, GHz	18.7	22.2	33	36.5	42	48	52-57	91.65	183.31
Amount of channels	2	1	2	2	2	2	5	2	3
Polarization	V,H	V	V,H	V,H	V,H	V,H	V	V,H	V
Resolution, km	75	68	45	41	36	32	30	18	12
Pixel size, km	32	32	32	32	32	32	64	16	64
Sensitivity in a pixel, K	0.25	0.25	0.35	0.38	0.45	0.45	0.3	0.5	0.4
Observation angle	51.3°								
Incidence angle	65°								
Swath width, km	2600								
Scanning	conical								
Scanning period, s	2.5								
Mass, kg	107								
Power consump., W	110								

3.2. Algorithms for geophysical parameters

3.2.1 Development of retrieval algorithms for Aqua AMSR-E and ADEOS-II AMSR

Global and regional algorithms to retrieve SST t_S, wind speed W, total atmospheric water vapour content V and total cloud liquid water content Q were developed using numerical experiments with a model of microwave radiative transfer in the ocean-atmosphere system and database of oceanic and atmospheric parameters collected by research vessels in the World Ocean (Mitnik and Mitnik, 2003). The characteristics of the database are summarised in Table 6.

Table 6. Characteristics of a "core" database used for computation of the simulated brightness temperatures at AMSR/AMSR-E frequencies

Parameter	**Sea surface temperature ts (°C)**		**Wind speed W (m/s)**		**Total water vapor content V (kg/m^2)**		**Total cloud liquid water content Q, (kg/m^2)**	
Range	**- 1.6 + 31**		**0 – 30**		**2.4 – 75.7**		**0 – 7.07**	
Subranges and number of radiosondes in the subranges	< 0	13	0 – 5	669	0 – 10	438	0.0	791
	0 – 5	331	5 – 10	877	10 – 20	383	0.0 – 0.3	850
	5 – 10	233	10 – 15	388	20 – 30	210	0.3 – 0.6	168
	10 – 15	260	15 – 20	107	30 – 40	118	0.6 – 1.0	105
	15 – 20	202	20 – 25	8	40 – 50	193	1.0 – 1.5	53
	20 – 25	98	25 – 30	1	50 – 60	473	1.5 – 3.0	49
	25 –3 0	839			60 – 70	229	> 3.0	34
	> 30	74			> 70	6		

Computations of the brightness temperatures T_B were carried out for AMSR/AMSR-E frequencies ν_i, i =6 (AMSR-E) and 8 (AMSR) with vertical (V) and horizontal (H) polarizations. Massifs of the simulated $T_B^{V,H}(\nu_i)$ and parameters t_S, W, V and Q were used for retrieval algorithm development.

3.2.2 SST and wind speed algorithms

Coefficients of linear regression equations were derived for t_S and W by statistical processing of the $T_B^{V,H}(\nu_i)$. Retrieval errors σ_{ts} and σ_W were computed at different combinations of t_S and variations of radiometer noises. Table 7 shows that the decrease of number of channels n from 10 to 5 results in the minor increase of t_S and W retrieval errors. However elimination of two additional channels is accompanied by the sharp increase of the errors even for ideal (without noises) radiometer.

Table 7. SST and wind speed retrieval errors at variation of number of channels

Number of channels	**a_o, °C**	**a_1**	**σ_{ts}, °C**	**b_o, m/s**	**b_1**	**σ_W, m/s**
10	**-0.002**	**1.0**	**0.160**	**0.028**	**0.997**	**0.250**
5	**0.007**	**1.0**	**0.191**	**0.024**	**0.997**	**0.280**
3	**-0.070**	**1.0**	**0.270**	**0.150**	**0.980**	**0.62**

$T_B^{V,H}$ at $\nu = 6.9$ and 10.7 GHz were used in t_S and W algorithms (4 channels). $T_B^{V,H}$ at $\nu = 6.9$ and one 10.7-GHz channel were used in 3-channel algorithms (Mitnik and Mitnik, 2003).
The values of t_S were retrieved by a formula:

$$t_S = A_o + A_1 T_B(6.9H) + A_2 T_B(6.9V) + A_3 T_B(10.7V) / T_B(10.7H) + A_4[(T_B 6.9V)]^2$$

The increase of t_S retrieval errors due to radiometer noises is evident from Table 8.

Table 8. Influence of radiometer noises on the SST retrieval errors

Noises $\Delta T(\nu)$, K		σ_{ts}, °C (3 channels)	σ_{ts}, °C (4 channels)
6.9 V, 6.9H	10.7V, 10.7H	6.9 V, 6.9H, 10.7V or 10.7H	6.9 V, 6.9H, 10.7V, 10.7H
0.0	0.0	0.26/0.37	0.15
0.1	0.13	0.40/0.43	0.40
0.2	0.27	0.67/0.58	0.58
0.3	0.40	0.94/0.76	0.76

The expected retrieval errors were determined using the measured noises. To eliminate the influence of heavy clouds and precipitation the cases with $T_B(10.7V) > 185$ K were removed. Comparison of the retrieved values t_S and W with "ground truth" values t_{SO} and W_O is shown in Figure 20.

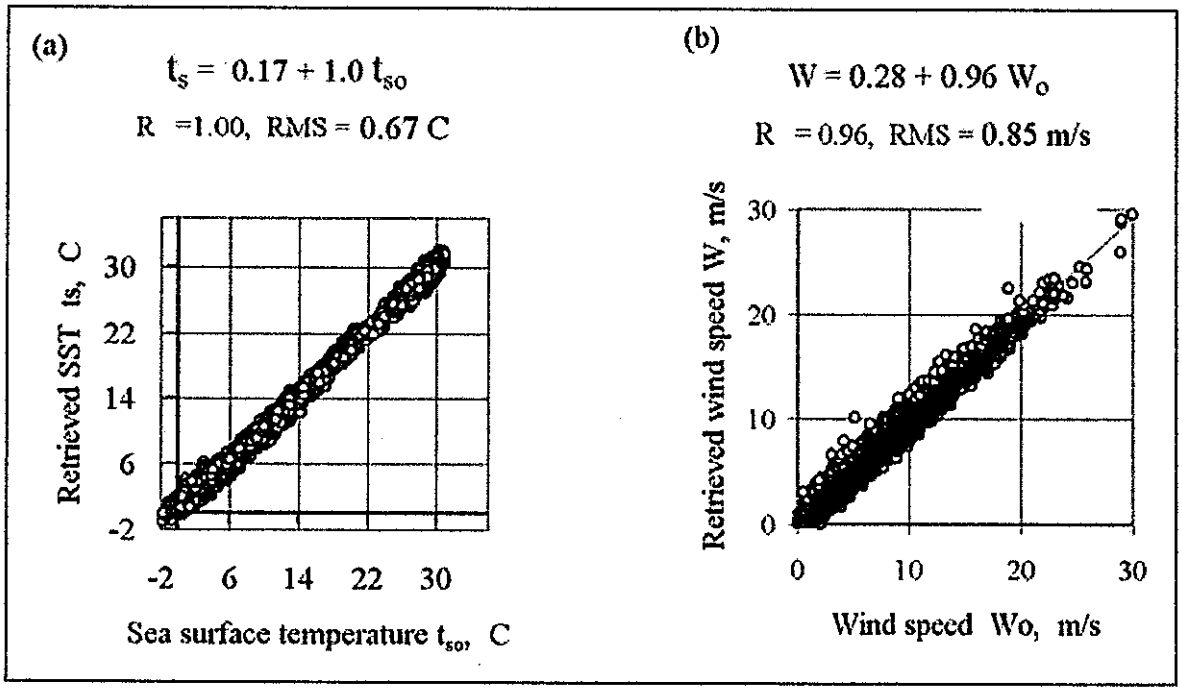

Figure 20. Scatter plots of the retrieved t_S and t_{SO} (a) and W and W_O for 3-channel algorithms at noises equal to 0.2 K (6.9-GHz channels) and 0.27 K (10.7-GHz channels) at $T_B(10.7V) < 185$ K. The strait lines are the best-fitting linear regressions.

3.2.3 Atmospheric water vapour content and cloud liquid water content

Physical-based global and regional (tropical and polar) algorithms were developed for retrieval of the integrated atmospheric parameters: total atmospheric water vapour content and total cloud liquid water content. The T_Bs at 23.8 and 36.5 GHz with vertical polarization and SST values are used in the algorithms. (It is supposed that SST values are derived from T_Bs at 6.9 and 10.7 GHz – see 3.2.2). Retrieval errors are equal to about 2 kg/m^2 for V and about 0.025-035 kg/m^2 for Q (Figure 21) (Mitnik and Mitnik, 2003).

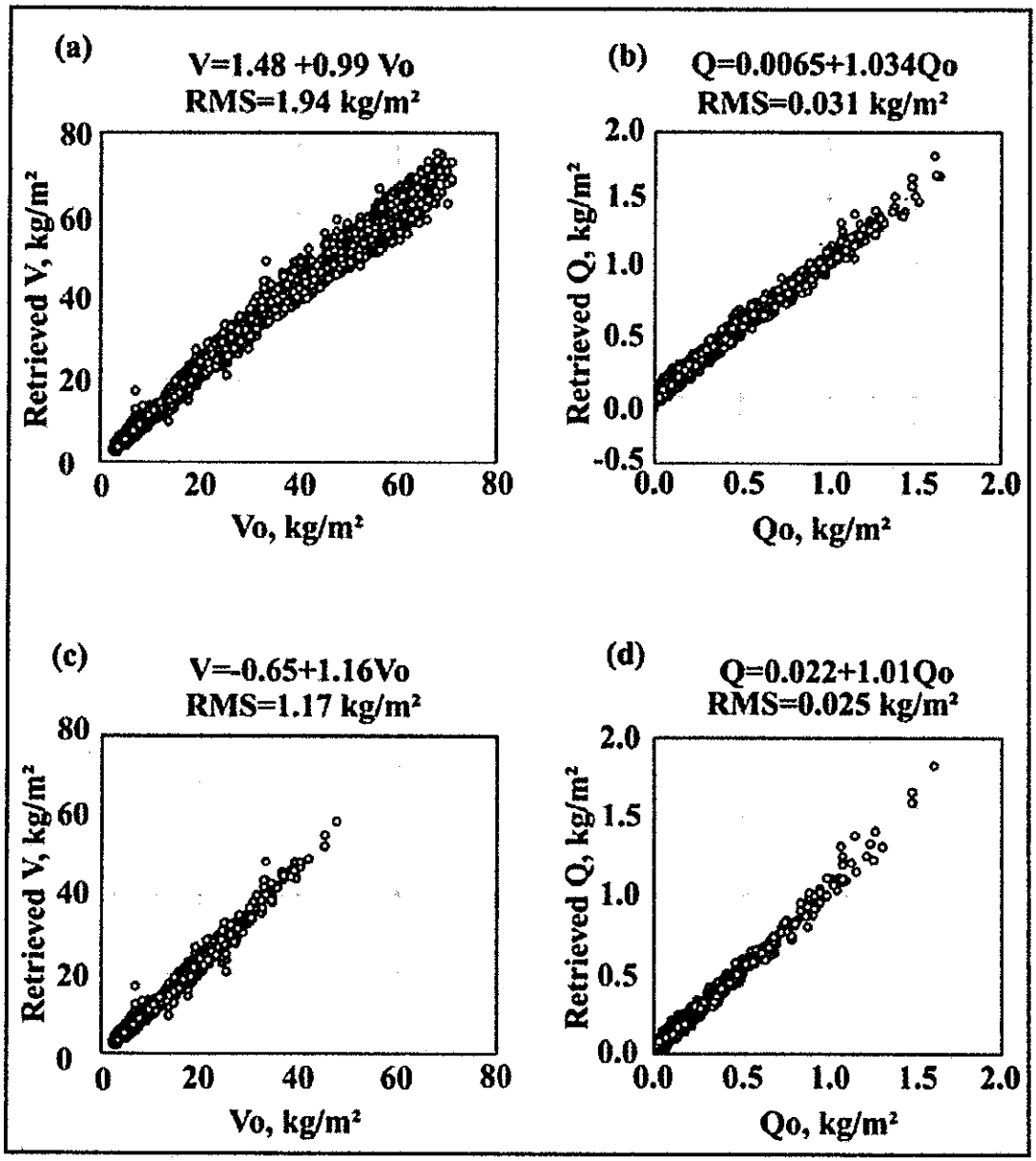

Figure 21. Scatter plots of the retrieved and radiosonde-derived values of total water vapor content and total cloud liquid water content for global (a) and (b) and polar (c) and (d) databases computed at radiometer noises ΔT(23.8V) and ΔT(36.5V) = 0.5 K and σ_{ts} = 1.0°C. Polarization difference $\Delta T36 = T_B(36.5V) - T_B(36.5H) \geq 20$ K. The strait lines are the best-fitting linear regression (Mitnik and Mitnik, 2003).

Retrieval errors of geophysical parameters can be decreased by application of neural networks-based algorithms (Zabolotskikh et al., 2000; 2004). Numerical experiments allowed estimating optimal architecture of neural network (number of hidden layers and neurons).

3.3. Validation of geophysical parameters

Aqua AMSR-E and ADEOS-II AMSR measurements were provided by the Japan Aerospace Exploration Agency (JAXA) within the cooperation between the JAXA and the POI FEB RAS in the ADEOS-II Research activity (project A2ARF006).

The measured brightness temperatures T_Bs represent the binary data in hdf format. They were transferred in text files for subsequent processing. Application of the developed algorithms (Mitnik and Mitnik, 2003) to T_Bs have shown that there are discrepancies between the retrieved and ground truth values of parameters caused very likely by calibration errors. Histogram technique based on a comparison of histograms of the simulated and measured brightness temperatures was suggested to reveal the calibration errors (Mitnik, 2004). The errors were detected, the corrections ΔT_B to the T_Bs were estimated and the corrected versions of the retrieval algorithms were developed. ΔT_B values were different for different channels and were equal to 0.5-4 K.

Corrected 4-cannel t_S algorithm is given by the following equation:

$$t_S = A_o + A_1[T_B(6,9V) + \Delta T_B] + A_2 T_B(6,9H) + A_3 T_B(10,7V) + A_4[T_B(6,9H)]$$

where ΔT_B = 1.5 K and coefficients A_i, i = 1,...,4 were also slightly changed compare to the initial version.

Match up data sets were prepared by the JAXA and provided to Principal Investigators (PIs) via ftp. They consist of massifs of collocated in space and close in time the AMSR/AMSR-E T_Bs and

- SST and wind speed and direction values measured by oceanic buoys and by ships and
- radiosonde reports.

The t_S values retrieved with the corrected algorithm are in a good agreement with ground truth data. The results of comparison for match up data set for 26 October 2003 are presented in Figure 22.

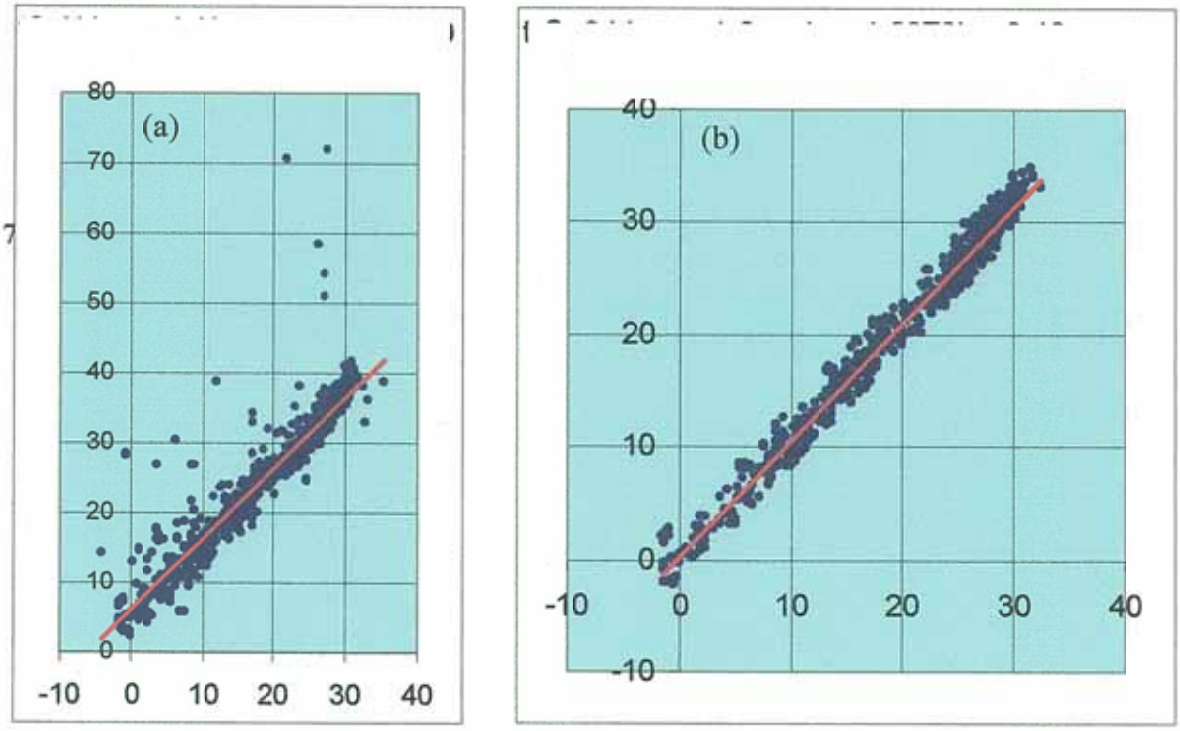

Figure 22. SST retrieval from AMSR-E data taken on 26 October 2003. Comparison with *in situ* data. Global algorithm.

All points (n = 994) of match up database for 26 October 2003 are shown in Figure 22a. The corresponding linear regression equation is $t_s = 5.9 + 1.01t_o$ and root mean square (rms) of the retrieved SST values $\sigma_{ts} = 3.44^{\circ}C$. After application of flags (to exclude cases with precipitation as well as erroneous T_Bs measurements), 150 points were removed the regression equation became as $t_s = 0.13 + 1.0378t_o$ and rms error decreased till 1.2°C (Figure 22b). In reality this error can be further decreased if preliminary classification of satellite – *in situ* data will be done in accordance with physical mechanisms influencing both on the retrieved and *in situ* SST values: time (day or night), wind speed (low-moderate or high) etc.

These match up data sets were used to correct (tune) the retrieval algorithms for all geophysical parameters, to modify slightly coefficients of regression equations and estimate the retrieval errors. Some problems in AMSR and AMSR-E data calibration were revealed. They were discussed at the ADEOS-II PI Workshops (Tokyo, 1-3 March 2004 and Nagahama, 8-10 December 2004, http://sharaku.eorc.jaxa.jp/ADEOS2/ws_nagahama/). The T_Bs are reprocessed using corrected calibration dependencies. The corrected T_Bs can be used by PIs on the basis of "Announcement of EOIC online Service User Approval".

Now comparison of retrieved and *in situ* data can be performed everyday using POI GIS. User selects the area and period of observations and uses GIS to download both the available AMSR-E data and *in situ* observations of the SST and wind speed and direction. The GIS extracts this data from its databases and also from NEAR-GOOS project database. The former contains the data collected on NEAR-GOOS site through Global Telecommunication System. Then user calls up the t_S and W retrieval algorithms from the GIS analytical support system. The retrieved t_S and W fields are displayed in map windows of GIS. Retrieval errors are computed by comparison of the satellite-derived and *in situ* values for each algorithm under investigation (Golik et al., 2004a,b).

Example of validation of the corrected 4-channel t_S retrieval algorithm for 2 January 2004 is shown on a POI GIS page (Figure 23). 125 NEAR GOOS buoy and ship t_S measurements carried out between 12 to 18 UTC were found within AMSR-E swath between 26-46°N, 128-142°E. Rms error was 1.25°C for all data without application of flags.

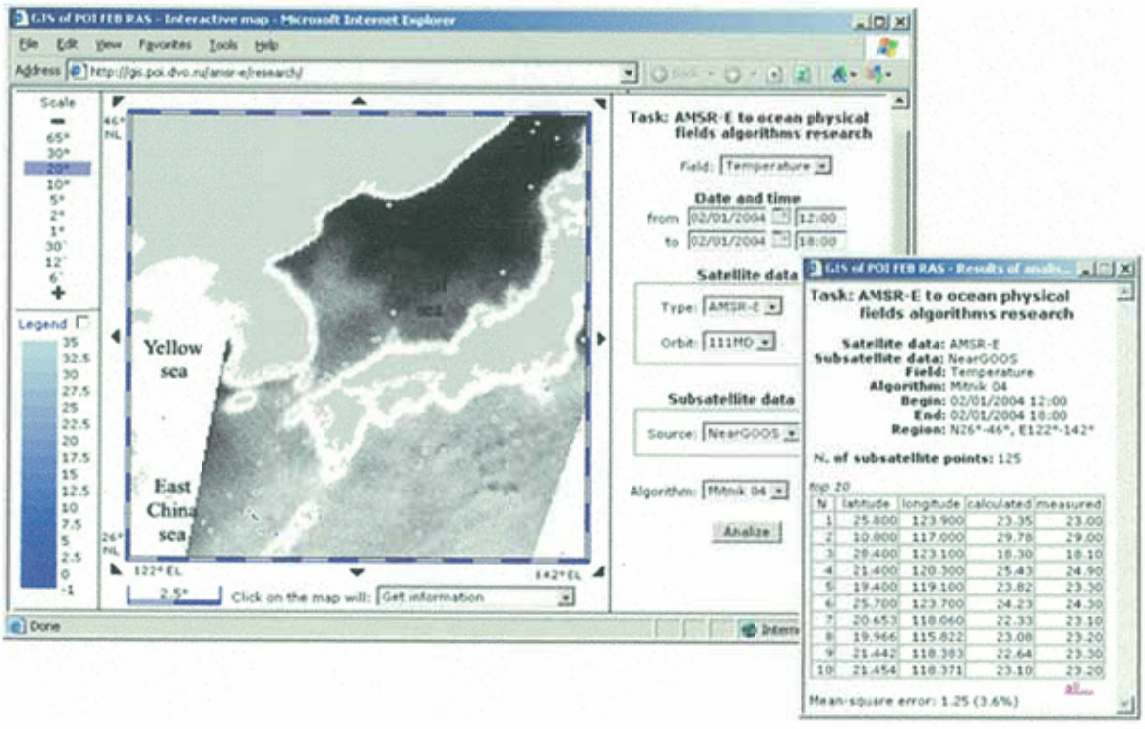

Figure 23. Validation of SST retrieval algorithm using AMSR-E, NEAR-GOOS and GIS POI

Interrelations of the simulation and satellite experiments, retrieval algorithms, retrieved and *in situ* data in the problem of construction of fields of the oceanic and atmospheric parameters from Aqua AMSR-E measurements illustrates Figure 24. Quantitative estimates of geophysical parameters were obtained for various marine weather systems (Mitnik, 2004; Mitnik et al., 2004c). Fields of brightness temperature at 89.0 GHz with horizontal polarization, total water vapor content V and total cloud liquid water content Q in a cyclone centered over the sea are shown in Figure 25.

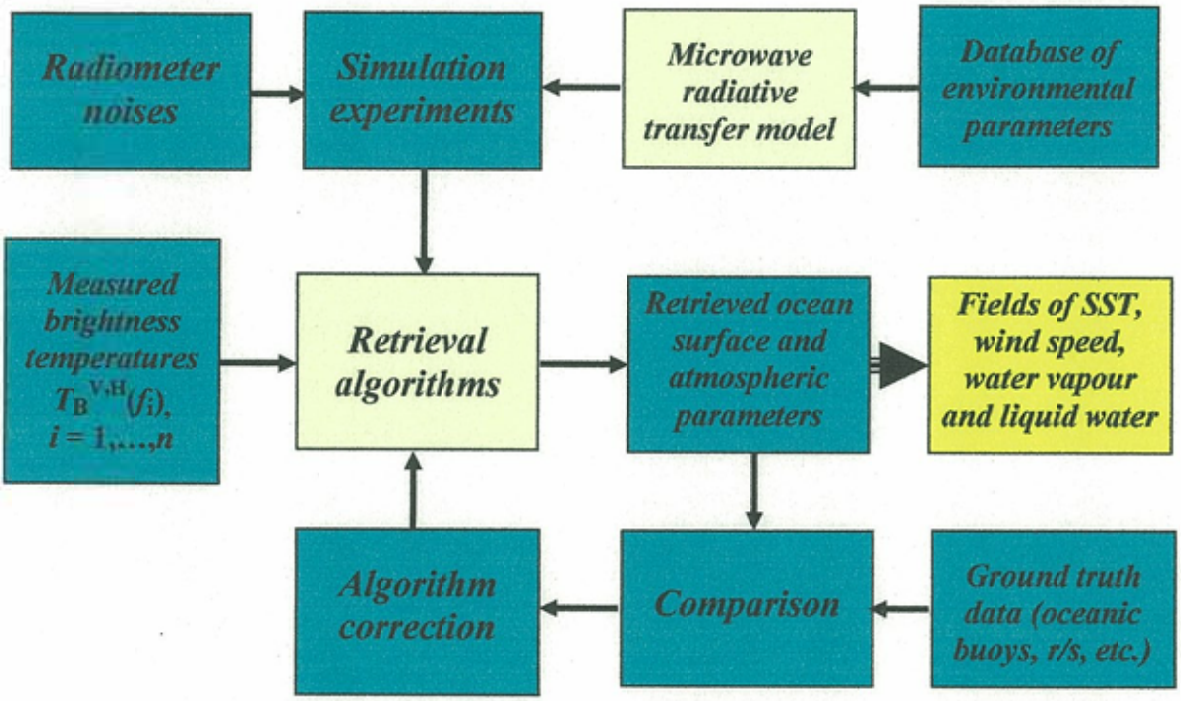

Figure 24. Schematic representation of the methodology used in development, tuning and validation of AMSR-E retrieval algorithms.

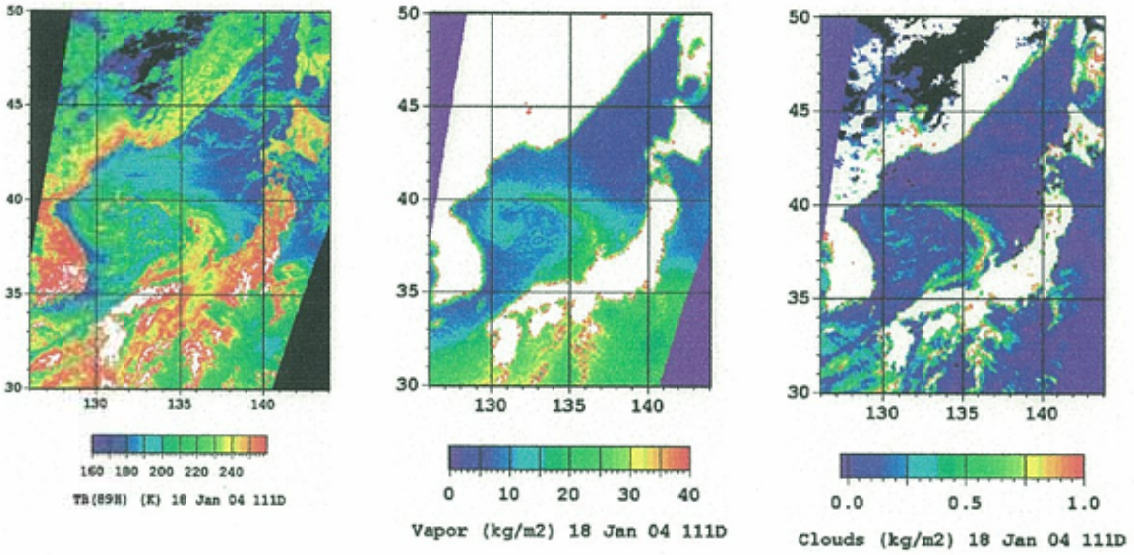

Figure 25. Brightness temperature at 89 GHz, H-pol, total water vapor content and total cloud liquid water content over the sea retrieved from Aqua AMSR-E measurements for 18 January 2004

4. INTRODUCTION OF LATEST FINDINGS

4.1 Mean monthly distributions of bio-optical characteristics in the NOWPAP region

A peculiar feature of the NOWPAR region between Russia, Korea and Japan consists in the presence of a clearly manifested frontal zone dividing the sea into two parts with different systems of currents. The boundary between them is the Polar Front; the temperature increment between the regions located north and south of the front (at 43° and 38°N) reaches 10°C in the winter and 5°C in the summer. A real position of the Polar Front is changeable and can be traced by NOAA AVHRR data. Dynamic features in the frontal zone are delineated on SAR images (Dubina and Mitnik, 2004).
Monthly coverage of the regions by satellite data in different months and years from January 1998 to December 2002 is near 100% from April to October; it reduces in the winter months.

The available data of field measurements show that the operational algorithm OC4 and the simplified algorithm for the particle backscattering coefficient provide quite reasonable results in this part of the NOWPAP region. Application of OC4 may be explained by the absence there of a significant riverine runoff delivering yellow substance and suspended matter. The semi-analytical algorithm for the yellow substance absorption coefficient a_g is not applicable here due to great errors in the atmospheric correction there. The simplified semi-analytical algorithm for a_g has been specially developed for this area. It is based on the use of the values of the normalized water-leaving radiance $L_{WN}(510)$; chlorophyll a concentration Chl a and the particle backscattering coefficient b_{bp} calculated from the SeaWiFS data; the analytical formula (Lee et al., 1998) relating $L_{WN}(510)$ to the parameter

$$L_{WN}(510) = b_b(510)/[a(510)+b_b(510)],$$

where $a(510)$ and $b_b(510)$ are the coefficients of seawater absorption and backscattering; the low-parametric models for spectral seawater absorption and backscattering (Kopelevich, 2001). Results of the algorithm validation with in situ measured data showed that the standard error is equal to 0.022 m^{-1} which is quite acceptable for the estimating calculations.

The prepared colour maps show the mean monthly distributions of chlorophyll a concentration and of the particle backscattering and the yellow substance absorption coefficients derived from SeaWiFS data by the above-mentioned algorithms from January 1998 to December 2002. Figure 26 shows monthly maps of chlorophyll a concentration in 2001 and Figure 27 – monthly maps of the yellow substance absorption coefficient in 2000 (Kopelevich et al., 2003).

It can be seen from analysis of all data that the most seasonal changes occur in March-June, during the period of the spring phytoplankton bloom, which first covers the southern part of the sea and then the northern part. In October - December the autumn phytoplankton bloom is observed. The distributions of the particle backscattering and the yellow absorption coefficients change similarly but with no pronounced autumn maxima.
The pronounced seasonal changes are seen in 1998-2002 in all bio-optical characteristics and they are similar in the different years. The changes of different characteristics are also similar, and it can be suggested that variability of the bio-optical characteristics is mainly determined by its bioproductivity and the climatic factors.

Some effects of the local sources of the suspended and colour dissolved organic matter on the distributions of the particle backscattering and yellow substance absorption coefficients should be noted. One can see from the maps that the distinction of the seasonal changes in the b_{bp} values in the southern half of the sea from all other seasonal distributions including the b_{bp} seasonal changes in the northern half. This is explained, in particular, by the fact that the b_{bp} values in the southern half in the fall-winter season are significantly greater than those in the northern half. The distinction is presumably caused by the precipitation of the aerosol particles driven by the monsoon winds from the Gobi Desert mostly across the southern part of the sea.

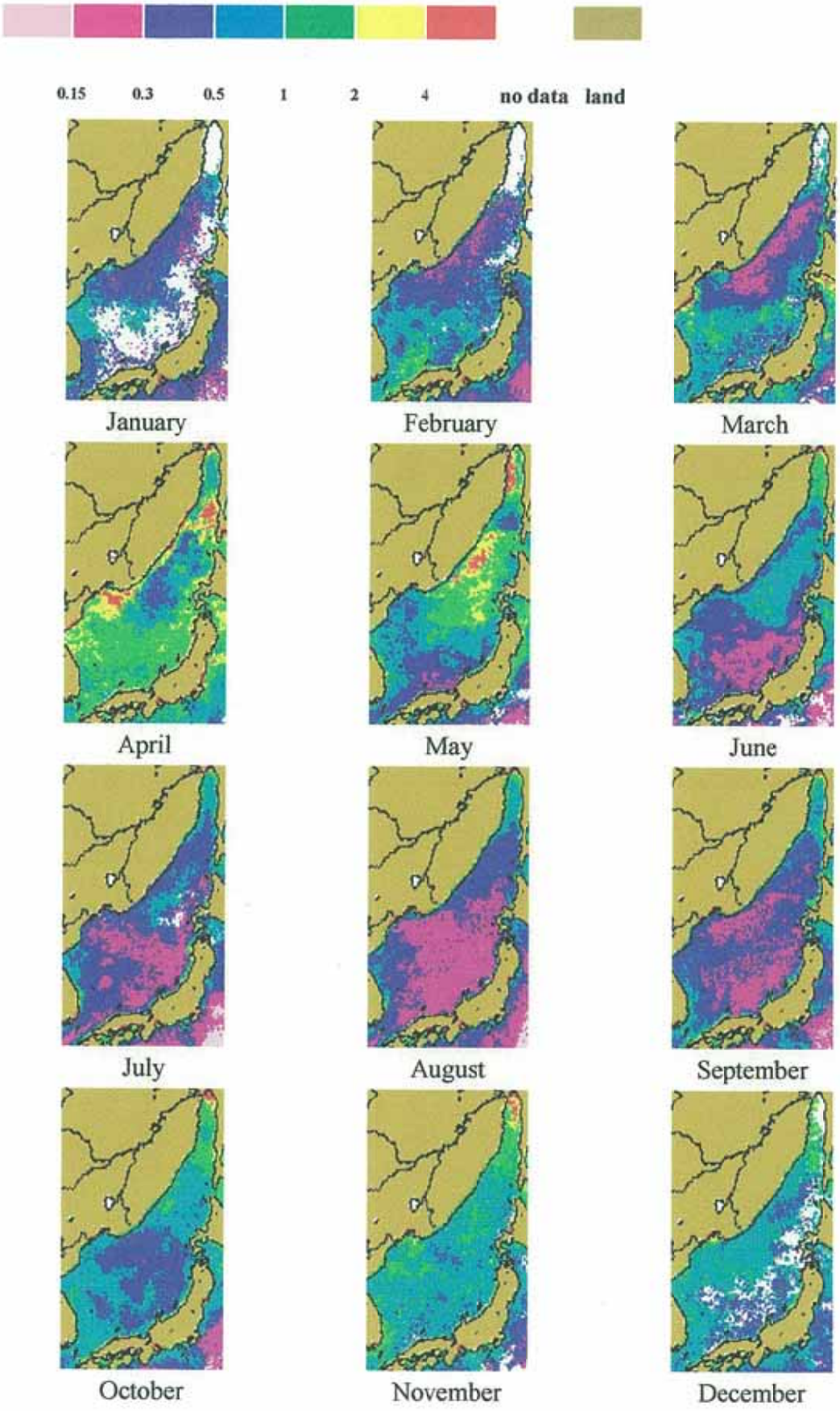

Figure 26. Maps of mean monthly values of chlorophyll *a* concentration (mg/m^3) in 2001.

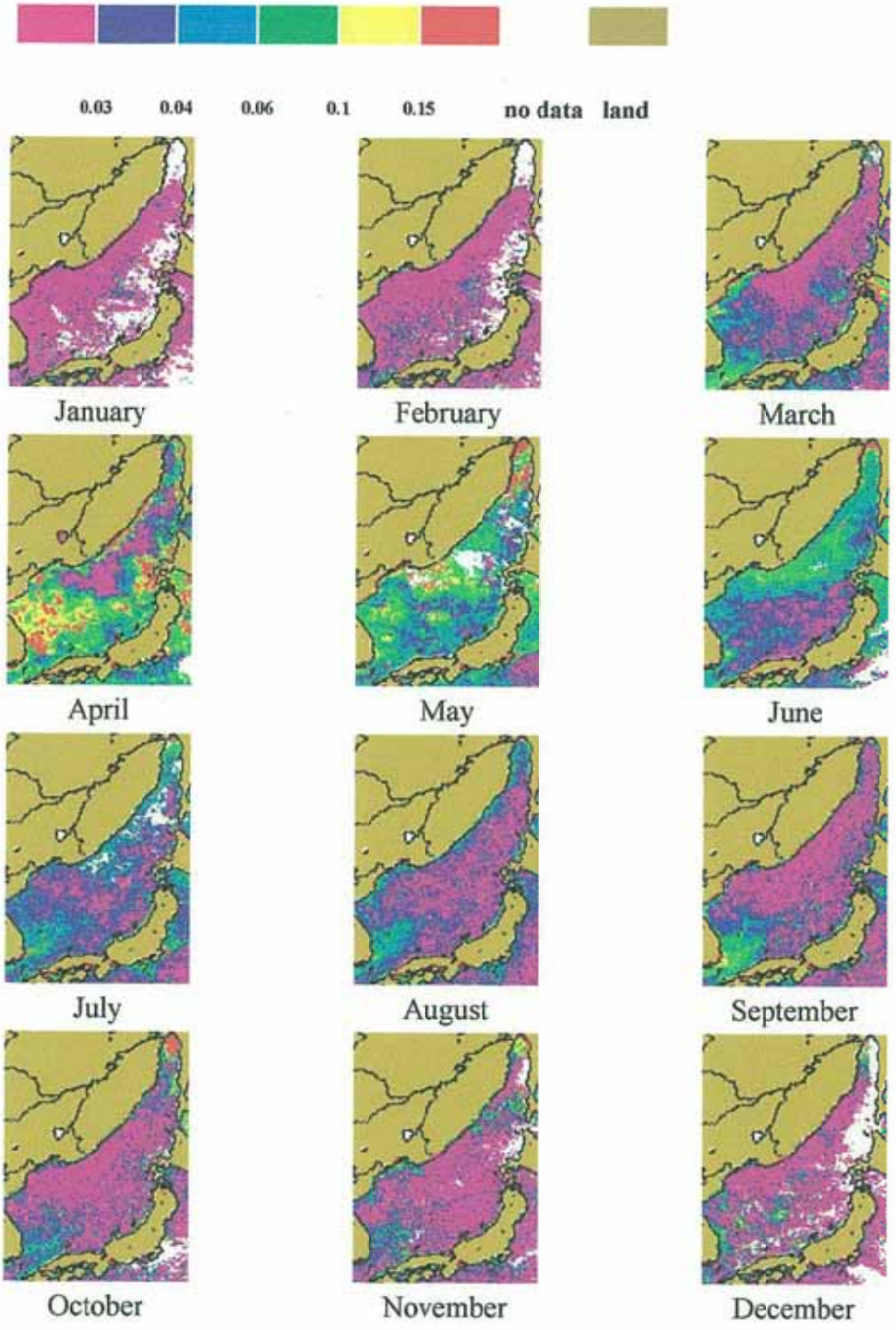

Figure 27. Maps of monthly mean values of yellow substance absorption coefficient in 2000

In the southern half of the sea the seasonal changes in b_{bp} and a_g feature additional peaks in July-August, which are not observed in the seasonal distributions of the chlorophyll *a* concentration. The above maxima may be caused by the plume of Yangtze River reaching the region under consideration from the East China Sea via the Korea Strait.

In Table 9 are given the mean annual values of chlorophyll *a* concentration and of the particle backscattering and the yellow substance absorption coefficient as well as their standard deviations in 1998-2002. It is seen that the least values of all characteristics were in 1998. The highest values of chlorophyll *a* concentration were observed in 2000, of the particle backscattering coefficient in 2002. The interannual changes of the yellow substance absorption were within accidental deviations.

The annual means of b_{bp} and a_g in the northern and southern halves of the sea coincided closely with each other. Chlorophyll *a* concentration in the northern half was higher than in the southern one in all years but the difference was significant (with the level of significance of 0.05) only in 2000 and 2001; in other years it was within accidental deviations.

Table 9. The annual mean values of chlorophyll *a* concentration, the particle backscattering coefficient, and the yellow substance absorption coefficient with their standard deviations in the northern and southern halves of the sea derived from SeaWiFS data in 1998-2002

Year	Northern half	Southern half	Whole basin
	Chlorophyll *a* concentration, mg m^{-3}		
1998	0.76±0.39	0.65±0.24	0.71±0.29
1999	0.84±0.40	0.77±0.32	0.81±0.34
2000	0.91±0.31	0.78±0.32	0.84±0.29
2001	0.86±0.43	0.70±0.29	0.79±0.34
2002	0.81±0.31	0.76±0.33	0.78±0.31
1998-2002	0.83±0.36	0.73±0.29	0.79±0.31
	The particle backscattering coefficient x 10^3, m^{-1}		
1998	3.3±1.3	3.5±0.4	3.4±0.8
1999	3.5±1.4	3.7±0.6	3.6±0.9
2000	3.9±1.1	3.6±0.5	3.8±0.7
2001	3.7±1.5	3.8±0.5	3.7±0.9
2002	4.2±1.3	4.5±0.6	4.3±0.9
1998-2002	3.7±1.3	3.8±0.6	3.8±0.9
	The yellow substance absorption coefficient, m^{-1}		
1998	0.037±0.029	0.038±0.014	0.038±0.021
1999	0.041±0.028	0.046±0.024	0.044±0.025
2000	0.043±0.022	0.045±0.020	0.044±0.020
2001	0.043±0.034	0.044±0.022	0.043±0.028
2002	0.040±0.027	0.048±0.024	0.044±0.025
1998-2002	0.041±0.028	0.044±0.021	0.042±0.023

4.2 Space monitoring of ice cover for routine mapping and long-term investigations

Scientific Research Centre (SRC) "Planeta" developed technology for routine mapping and of ice cover as well as for study its long-term characteristics by processing of the current and archive satellite information. Construction of ice condition maps is carried out with the usage of multifunction PlanetaMeteo program system (Trenina, 2004). The construction includes several steps. At first the base of a map is created by specification of the following characteristics:

- geographical coordinates of the region
- type of projection (stereographic)
- resolution (m/pixel)
- geographical map spacing
- font

Information for construction of the vector maps (coast line, rivers, etc.) is also provided.

The visible, infrared and radar images obtained from "Meteor", "Resurs" and "Okean" (Russa) and from NOAA, Terra and Aqua (USA) are used for ice condition mapping. Most of the data is derived from NOAA AVHRR observations. Various transformations can be done with input AVHRR data:

- Selection of any combination of spectral channels
- Display of synthesized color
- Image scaling in accordance with window scale
- Automatic scrolling of the image
- Automatic or interactive image contrasting with different transfer function.
- Removing of geometric distortions, transferring in stereographic projection of the given region, etc.
- Automatic import description of raster map parameters.
- Automatic creation of multilayer raster (image + cartographic base), etc.

The raster layers can be combined in any order and shifted independently of one another. Raster with maximum sizes is used as a basis one.

The final step in technology of satellite data processing is thematic interpretation of ice cover parameters. It is performed by qualified specialist (interactive decoding). Accuracy and reliability of ice condition maps depend on specialist's experience. A great body of practical and expert knowledge cannot be formalized now such as analysis of climatic variability of ice characteristics in a given area, analysis of ice conditions obtained on the basis of satellite observations in the previous and current periods, analysis of hydrometeorological situation, etc.

The following ice cover characteristics are applied to the selected zones:

- Concentration (total and partial)
- Age
- Type

In the frame of routine activity, the SRC "Planeta" issues every year more than 600 maps-schemes and mosaics of ice conditions for the Arctic and Antarctic as well as for the Russian seas. Apart routine tasks, technology of ice cover mapping was used for various long-term projects;

Investigation of annual variability of ice cover in the western Arctic using a RAR installed on "Okean" series satellites.

Russian-European project ICEWATCH directed on routine mapping of ice conditions along the Northern Route using joint processing of the Okean RAR and ERS SAR images.

Estimation of the changes of the first year and multiyear ice areas and ice cover dynamic in Arctic using the multiyear archive of the RAR images acquired from Okean series satellites.

The PlanetaMeteo program system was used also

- to construct the ice conditions maps in Tartar Strait,
- to investigate the space-time characteristics of ice in the Nevelskoy Strait,
- to isolate the vast floes on satellite images (examples are given in Figure 28 and quantitative estimates in Table 10).

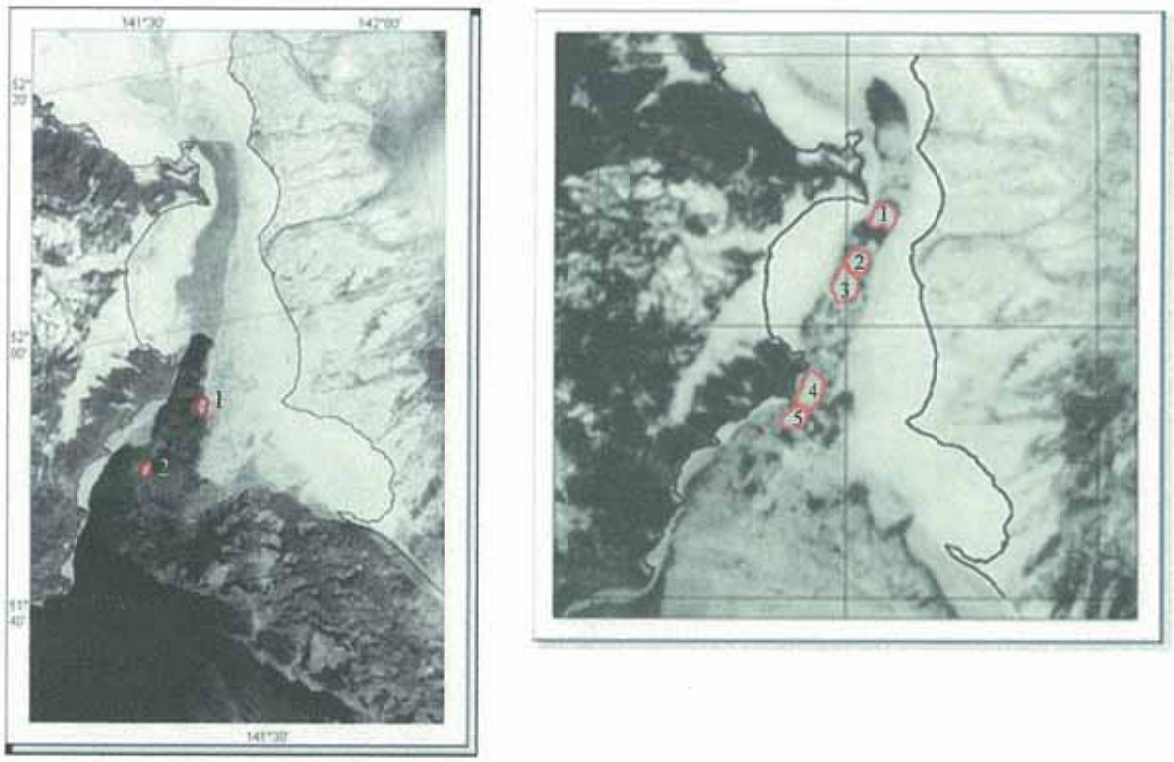

Figure 28. Isolation of vast floes in the Tatar Strait on satellite images acquired by a camera MK-4 on 6 February 1989 from Resurs-F satellite (left) and by Multiband Scanning Unit of Medium Resolution MSU-M on 19 January 1990 from Okean-O1 satellite (right)

Table 10. Maximum linear size and area of the vast floes shown in Figure 26

Resurs-F, camera MK-4, 6 February 1989			*Okean-O1, MSU-M, 19 January 1990*		
Vast floe	Maximum linear size (m)	Area (km^2)	Vast floe	Maximum linear size (m)	Area (km^2)
1	2702	2.906	1	3960	8.395
2	2492	1.950	2	3360	1.950
			3	4800	10.469
			4	5400	11.736
			5	3840	6.278

4.3 Oceanic fronts in the Southern Indian Ocean

Weekly the NASA Ocean Data System/Multi-Channel Sea Surface Temperature) dataset was used to investigate detailed structure and space-time variability of large-scale fronts in the Southern Indian Ocean (30-60°S and 20-150°E) during the period of 1997-1999. The constructed SST gradient maps 36 mid-month weeks gave simultaneous viewing of five basic fronts in the whole basin: the North and South Subtropical fronts, the Agulhas Front, the Subantarctic Front, and the Polar Front. Mean location, SST and SST gradients with corresponding standard deviations were calculated for every front at each 10°-spaced longitude. SST gradient maps and charts of sea level anomalies (SLA) based on the combined altimetry data from the TOPEX/Poseidon and ERS-2 satellites, as well as corresponding charts of sea surface dynamic heights (constructed by the superposition of SLA distributions over the climatic dynamic topography), were used to study mesoscale variability related to the fronts. The analysis allowed to distinguish zones of enhanced meandering (eddy formation) with amplitudes of 2°-5° in latitude and wavelength of several degrees in longitude, and their relationship with bottom topography peculiarities. Double structure of fronts and close approach of neighboring fronts appear in different areas of the basin (Kostianoy et al., 2004b).

The fields of sea level anomalies (SLA) were constructed at the Department of Satellite Oceanology (Collecte, Localisation, Satellites – CLS) at the Center National d'Etudes Spatiales (French Space Agency – CNES). The T/P and ERS data were united in time intervals corresponding to the cycles of the T/P satellite. In addition, the charts of sea level anomalies issued at the Colorado Center for Astrodynamics Research (CCAR), USA, based on the combined data of the T/P and ERS-2 altimeters we used. The error in the SLA altimetry (~3 cm) is significantly smaller then the dynamic height anomalies related to the meanders (eddies) in the southern part in the Indian Ocean (10 – 30 cm, (Park and Gamberoni, 1995)).

This allowed us to compare the altimetry data with the quasi-synchronous charts of the SST gradients (fronts) on the basin scale, which was obtained from the MCSST data for the same period and with the same periodicity. The SLA charts distinguish the regions of the most intensive mesoscale variability in the basin, while the corresponding dynamic ocean level charts and charts of the SST gradients provide the information on the position of the meandering fronts and their branches, their interaction, and peculiarities of the large-scale circulation in the basin.

The synoptic altimetry charts distinguish an interesting peculiarity of the frontal dynamics: the streamlines corresponding to a certain front easily pass from one branch of the front to another or separate from the front merging with a neighboring front and later returning to the initial front.

The possibility and efficiency of using regular all-weather high-precision combined data of the TOPEX/POSEIDON and ERS-2 altimeters to study the structure and dynamics of the fronts in the southern part of the Indian Ocean and the mesoscale variability related to the fronts was demonstrated. The high spatial resolution, together with the uniform coverage of the entire basin with the data, allows obtaining synoptic charts of the ocean dynamic level on the entire ocean scale on their basis, which indicates a significant advantage of the altimetry information as compared to the hydrographic surveys. Such altimetry information can be used not only for mapping the fronts and eddies but for tracing the pathways of eddy migration, as well as analyzing the hydrographic measurements. Joint application of the quasi-synchronous altimetry charts of the ocean level and the satellite SST (and SST gradients) charts is effective. This allows to relate the closeness of the streamline to a certain front, since the ranges characteristic of the main fronts in the southern part of the Indian Ocean are currently known (see references in Kostianoy et al., 2004b).

5 STRATEGIES / PLANS FOR RS RELATED ACTIVITIES

5.1 Technology of information system construction for access to satellite data in receiving centers of Federal Service on Hydrometeorology and Environmental Monitoring

Information system "Sputnik" is under development in Scientific Research Center (SRC) "Planeta" since 1997 (*http://sputnik.infospace.ru*). It is joint project of SRC "Planeta" and Space Research Institute (IKI RAS). It is supported by Division of ground microprocessor information systems of SRC "Planeta" and Space Monitoring Information Support (SMIS) Laboratory of IKI RAS. The system aims (предназначена) mainly for organization of work with different archives of raw satellite data. The main task of "SPUTNIK" server is to provide information about Russian weather satellites.

Information about the following satellites can be found:

- Geostationary weather satellite "Elektro" (GOMS) (till 13 Aug 1998).
- Space System "Meteor-3M"
  Space Ocean Sensing System Okean-O
  Space Remote Sensing System Resurs

Beyond Russian satellites, these centers receive and process information from NOAA series satellites and geostationary weather satellites.

The system also provides access to information products obtained at satellite data processing. Fully automatic complexes for receiving, processing and presentation of satellite data were produced. These complexes are used in particular to process data taken by TERRA and AQUA MODIS. These complexes are under construction in Western-Siberian (Novosibirsk) and Far Eastern (Khabarovsk) Centers of receiving and processing of satellite data (Lupyan et al., 2004; Asmus et al., 2004).

5.2 Technological structure of fishery monitoring system in Far Eastern region

System of fishery monitoring to control fisheries in the Far Eastern region was created. The system is a part of common to all-branch monitoring system and includes three subsystems: environment, fishery objects and fishery fleet. There are specific features in monitoring of the objects of these subsystems and thus it was important to maintain their hardware and software compatibility. To maintain solution of broad spectrum of problems technology of management and support of common information resource was realized. Satellite observation is the central part of the system. The basic sources of information in the system serve meteorological satellites NOAA, which permit in addition to the images of cloudiness and land surface to get after processing maps of sea surface temperature and ice conditions; satellites NavStar (GPS), responsible for accurate coordination of ships; satellites Inmarsat, maintaining information exchange between fishery ships and the monitoring center.

In Far Eastern region, the system includes the monitoring center KCSM, supplying data gathering and commutation center of the Space Research Institute responsible for information transfer to information nodes of users of the monitoring system. Technically, the system is an assemblage of software-hardware and the systems for automatic data receiving, processing, storage and distribution. It includes: telecommunication system, computer complex, general-system and applied software means (Protsenko et al., 2004).

5.3 Processing and using of polar orbital satellites Feng Yun

MVISR radiometer installed on polar-orbiting satellites Feng Yun-1C, Feng Yun-1D supplies images with a resolution of 1.1 km at 10 spectral channels five of which correspond to NOAA/AVHRR channels. Four additional channels are visible and one – infrared. Characteristics of MVISR channels allow to use them for retrieval of sea surface temperature and chlorophyll *a*

concentration. Spatial mismatch of the channels, the absence of calibration and noise filtration procedures in infrared channels, as well as the absence of algorithms of chlorophyll *a* estimate are the features which hamper usage of their data.

The following results were obtained by analysis of satellite information:

1. Angles orientation was determined for sensors of all channels and a method of geolocation was tested.
2. Chlorophyll *a* concentration was derived by using algorithm like to that developed for SeaWiFS. Comparison with the estimates obtained from SeaWiFS data have shown that Feng Yun-1D data can be used for chl *a* retrieval.
3. Calibration of IR channels was performed by using a procedure identical to that for NOAA KLM. Intercalibration of the Feng Yun and NOAA infrared channels allowed to determine the polynomial coefficients for calculation of black body temperature. Parameters of nonlinear correction were found (Alexanin et al., 2004b).

5.4 Ecological monitoring from Russian segment of International Space Station

"Uragan" (Hurricane) program devotes to monitoring of the land surface for natural resources study, environment protecting and tracing for dynamics of natural and technogenic from Russian segment of International Space Station (ISS). The program is carried out since January 2001, from the first days of new century. Scientific supervision of the "Uragan" program is handled by the Geographical Institute of the Russian Academy of Sciences.

Program consists of digital photography with a resolution up to 5 m and video survey. Information is storages at a hard disk. A part of data can be transfer to the Center of Flight Control immediately after survey. Only Russian cosmonauts conduct the survey since they study the fundamentals of the Earth Sciences and special preparation in accordance with survey program of the future flight. The main tasks are determined by a record book. Cosmonauts work with constant support by experiment producers.

The changes occurred in "Uragan" program since 2004. Before, the program was aimed to solve the scientific and methodological tasks. Now it is directed to solve the tasks formulated by administrations of different levels, state and private enterprises as well as by the scientific and educational centers. The analysis of the first results of space monitoring of natural and technogenic catastrophes including flooding, fires, pulsating glaciers, port's pollution, etc. has shown its high efficiency and necessity of cooperation with regional organizations. Program will last 10-12 years. (Kotlyakov and Desinov, 2004).

5.5 Coordination of activity in RS of environment

Pursuant to decision of III Intergovernmental Summit of the Remote Sensing of the Earth (Tokyo, April 25, 2004) is planned to create an international system of global observation of the Earth. For developing of the scientific concept and the programs of global monitoring of the Earth from space and pursuant to the disposal of Presidium of Russian Academy of Sciences # 10310-717 (August 11, 2004) Space Research Institute RAS and Center of Space Observations of the Russian Space Agency during November 16-18, 2004 conducted the Second Opened All-Russia conference "Current Aspects of Remote Sensing of the Earth from Space (Physical basics, methods and monitoring technologies of an environment, potentially of dangerous phenomena and objects)".

The second conference was conducted at participation of Institutes of Russian Academy of Sciences, Federal Services on Hydrometeorology and Environmental Monitoring, etc.
The directions of remote sensing related with monitoring of conditions of a land cover, ocean, atmosphere and vegetation were discussed on the conference on the following sessions:

A. Questions of creation and usage of satellite monitoring systems of a condition of the environment, natural resources, potentially of dangerous phenomena and objects.

B. Physical basics of methods of definition of the different environmental parameters, potentially of dangerous phenomena and objects with using of remote sensing data.

C. Methods, algorithms both technologies of processing and usage of the satellite information.

The first conference was held in Space Research Institute (IKI RAS) during November 10-12, 2003. 130 presentations and reports were submitted, 120 participants from 45 organizations have presented the plenary and sectional reported.

The third conference is planned to organize in Space Research Institute (IKI RAS) during November 2005.

6. CHALLENGES AND PROSPECTS

6.1 RS satellites under development

In accordance with Federal Space Program (2001-2005) Rosaviakosmos is responsible for making and launching of the following space apparatus: "Arkon", "Sich-1M", "Resurs-DK", "Resurs-01", "Meteor-3M" N2, "Electro", "Vulkan" and "Arkon-2" important for marine environment study. This family of satellites will allow fulfilling a national need for remote sensing information (http://www.rosaviakosmos.ru).

The Khrunichev State Research and the Production Space Center (http://www.khrunichev.ru) (Glazkova and Stefanofskiy, 2004) and NPO Mashinostroenia (http://www.npomash.ru) play a key role in development and construction of remote sensing satellites.

The Khrunichev State Research and Production Space Center plans to use a unified platform "Yacht" (Table 11) to make and launch the space apparatus "Monitor-E, -N, -C, -O, -R3, -R23" (Tables 12 and 13) for Earth's Remote Sensing

Table 11. Characteristics of a unified platform "Yacht"

Mass, kg	420
Power, kW	1...3
Orientation accuracy, deg	0.1
Stabilization accuracy, deg\sec	0.001
Expected operation duration, years	5...12

"Monitor-E" is planned to launch in August 2005 from Plesetsk launch site with a "Rokot" conversion rocket. "Monitor-E" represents new generation of space apparatus with improved characteristics. This space apparatus is designed for operational observations of Earth's surface within swath width of 90-160 km with a spatial resolution from 8 to 20 m. Instrument will carry out both panchromatic and multispectral survey of the underplaying surface and data transfer in near real-time regime. Its mass is 750 kg.

Table 12. Specification of space apparatus of "Monitor" system with radar

	"Monitor-R3"			"Monitor-R23"		
Range (wave-length), cm	X (3.1)			L(23.5)		
Polarization	VV, HH			VV+VH, HH+HV		
Spatial resolution, m	3-5	20/40	100/200	5-10	20/40	100/200
Swath width, km	10...20	30...80/120...160	400	20 - 40	60...80/120...160	300
Cover width, km	450			300		

Table 13. Specification of space apparatus of "Monitor" system with optic-electronic devices

	"Monitor-I" №1		"Monitor-I" №2		"Monitor-C"·		"Monitor-O"	
Spectral ranges	0.51-0.85 0.45-0.52 0.54-0.59 0.63-0.68 0.79-0.90	0.54-0.59 0.63-0.68 0.79-0.90	3.55-3.95 10.4-11.5 11.5-12.6	0.54-0.59 0.63-0.68 0.79-0.90	(stereo-module) 0.51-0.85	0.54-0.59 0.63-0.68 0.79-0.90	0.51-0.85 0.45-0.52 0.54-0.59 0.63-0.68 0.79-0.90	0.54-0.59 0.63-0.68 0.79-0.90
Spatial resolution, m	3(П); 6(МЗ)	20/40	60	20/40	4-5	20/40	1(П); 2(МЗ)	20/40
Swath (cover) width, km	36 (700)	160 (890)	160 (890)	160 (890)	65 - 70 (65 - 70)	160 (890)	20 (690)	160 (890)

NPO Mashinostroenia plans to make and launch *Kondor-E* satellite equipped by a S-band SAR with VV and HH polarizations. It is supposed that SAR will have two swaths (left and right) with a width of 500 km. Spatial resolution will varied from several meters to 100-150 m (scanSAR). Time of launching is TBD. http://www.npomash.ru/space/ru/space1.htm).

7 SUGGESTED ACTIVITIES FOR THE NOWPAP REGION

The following topics are under consideration as subjects for suggested activities.

Dissemination of projects' activities and results in the scientific community and the community of potential end users of remote sensing techniques considered and developed in the projects through workshops with potential users, public websites, information packages for interested scientists and users and newsletters.

In particular, the results on remote sensing of oil spills will be disseminated among the ongoing international projects concerning to the development of the system of operational monitoring of the NOWPAR region, (*titles of projects*) to fill existing gaps related to the early surveillance of oil pollution. Consultations with end users responsible for oil spill response and enforcement of environmental regulations in the NOWPAP region has revealed a number of barriers to the routine use of remote sensing data to monitor coastal pollution. These include a lack of awareness about the applications of satellite data to pollution monitoring, and lack of expertise in the interpretation of images. To address this problem the information about the state-of-the-art techniques developed by scientists in different countries will be disseminated by producing a teaching module on the remote sensing of oil spills and marine pollution. This will be made available on the Internet (in particular on CEARAC websites) and CD/DVD-ROM. Additionally, training and education courses on data fusion, SAR applications (oil spill monitoring, etc.) will be organized.

Demonstration to potential end users the possibilities and advantages of multisensor remote sensing techniques and obtaining information from the end users about their requirements (phenomena / parameters of interest, accuracy, resolution, coverage, economic constraints, etc.).

Multisensor remote sensing techniques will include:

- Analysis of the ERS-1/2, Envisat and ALOS Synthetic Aperture Radar, Envisat MERIS, NOAA AVHRR, ocean color, altimeter and scatterometer data collected over the NOWPAP region to study the surface manifestations of oceanic phenomena (currents, eddies, fronts, internal waves, upwellings), river/sea mixing zones, oil spills, sea ice and mesoscale regulated structures in the surface wind field important for coastal zone management and monitoring. (open sea and coastal frontal zones, East Korean Warm Current, Yangtze River mixing zone, coastal upwellings, etc.) to improve interpretation of the satellite images and to develop (semi)automatic techniques for classification of the oceanic and atmospheric phenomena.

- Analysis of the ADEOS-II AMSR, Aqua AMSR-E, NOAA AVHRR and other remote and *in situ* data obtained over the Northwestern Pacific Ocean to retrieve the sea surface wind, sea surface temperature, total atmospheric water vapor content, total cloud liquid water content and rainfall rate in the weather systems with gale winds and heavy precipitation (polar lows, cold air outbreaks, tropical cyclones and other) to reduce loss of life and property.

Exploitation of results in the context of operational remote sensing systems.

REFERENCES

Alexanin, A.I. and M.G. Alexanina (2004): Automatic revealing of eddies on satellite infrared images. In: *Actual problems of Space remote sensing of Earth.* E.A. Lupyan and O.Yu. Lavrova (Eds.) Moscow, Poligraph service Publishing House, 382-386 (in Russian).

Alexanin, A.I., M.G. Alexanina, D.A. Bolovin, F.E. Herbeck, A.V. Gromov, I.I. Gorin, Y.V. Naumkin, E.V. Fomin, Y.S. Epstain (2004a): Regional satellite monitoring of Far East Seas: Modern state and perspectives of development. *PICES Scientific Report.* No. 26. Proc. Third Workshop on the Okhotsk Sea and Adjacent Areas, S. McKinnell (ed), 81.

Alexanin, A.I., M.G. Alexanina, D.A. Bolovin, F.E. Herbeck, A.V. Gromov, Y.V. Naumkin, E.V. Fomin, Y.S. Epstain (2003): Satellite monitoring of Far Eastern seas. *All-Russia Conference "Actual problems of Space remote sensing of Earth",* Moscow, 10-12 November, 123 (in Russian).

Alexanin, A.I., S.E. D'yakov, A.V. Gromov, Y.V. Naumkin, and E.V. Fomin (2004b): Processing and using of polar-orbiting satellites FengYun. *Second Open All-Russian Conference "Actual problems of Space remote sensing of Earth*", Moscow, 16-18 November, 2004, 34 (in Russian).

Asmus, V.V., O.E. Milekhin, E.A. Lupyan, R.R. Nazirov, A.A. Mazurov, E.V. Flitman, A.A. Proshin, M.A. Burtsev, V.O. Il'in and V.Yu. Efremov (2004): Usage of technology of information system construction for access to satellite data in receiving centers of Federal Service on Hydrometeorology and environment monitoring. *Second Open All-Russian Conference "Actual problems of Space remote sensing of Earth*", Moscow, 16-18 November, 2004, 56 (in Russian).

Basharinov, A.E., A.S. Gurvich and S.T. Egorov (1974): *Microwave Emission of the Earth as a Planet* (*Radioizluchenie Zemli kak planeti*). Nauka Publiching House, Moscow, 187 pp. (in Russian).

Chernyavskiy, G.M. (2004): Problems of satellite monitoring of the Earth. *Second Open All-Russian Conference "Actual problems of Space remote sensing of Earth*", Moscow, 16-18 November, 2004, 27-28 (in Russian).

CleanSeas Overview. http://www.satobsys.co.uk/CSeas/viewframe.html

Danchenkov, M.A., et al. (1999): Oceanographic features of the LaPerouse Strait, In: *PICES Scientific Report No. 12,* 159-171.

Darkin, D.V., L.M. Mitnik and V.A. Dubina (2004): Statistics of SAF expressions in the Asian Marginal Seas on ERS-1/2 and Envisat SAR images. *Second Open All-Russian Conference "Actual problems of Space remote sensing of Earth*", Moscow, 16-18 November, 2004, 134 (in Russian).

DISMAR - Data Integration System for Marine Pollution and Water Quality. http://www.ucc.ie/ucc/research/crc/pages/projects/dismar.htm

Dubina, V.A. and L.M. Mitnik (2004): Investigation of surface circulation in the Japan Sea from satellite multisensor data. In: *Actual problems of Space remote sensing of Earth.* E.A. Lupyan and O.Yu. Lavrova (eds.) Moscow, Poligraph service Publishing House, 340-346 (in Russian).

Dubina, V.A., L.M. Mitnik and M.V. Mudriy (2003): Oil pollution of the Asian marginal seas: detection and possibilities of monitoring with the usage of satellite SAR. *All-Russia Conference "Actual problems of Space remote sensing of Earth",* Moscow, 10-12 November, 123 (in Russian).

Dubina, V.A. and L.M. Mitnik (2004): Evidence of the West Sakhalin Current in ERS-2 and Envisat-1 collocated SAR images. *Envisat & ERS ESA Symposium* (Salzburg, Austria, 6-10 September 2004), 6 pp

Ermakov, S.A. (2004): On possibilities of radar diagnostic of films on the sea surface. *Second Open All-Russian Conference "Actual problems of Space remote sensing of Earth"*, Moscow, 16-18 November, 2004, 135 (in Russian).

Ermakov, S.A., O.Yu. Lavrova, E.V. Makarov, I.A. Sergievskaya and Yu. B. Shchegolkov (2004): Field experiments on oil product dispersion and their radar sensing. *Second Open All-Russian Conference "Actual problems of Space remote sensing of Earth"*, Moscow, 16-18 November, 2004, (in Russian).

Fefilov, Yu.V. (2003): Information technology of remote determination of primary productivity in the systems of ocean monitoring. *All-Russia Conference "Actual problems of Space remote sensing of Earth"*, Moscow, 10-12 November, 123 (in Russian).

Frate, F. D., A. Petrocchi, J. Lichtenegger, and G. Galabresi. (2000): Neural networks for oil spill detection using ERS-SAR data. *IEEE Trans. Geosci. Remote Sens.*, 38, No. 5, 2282-2287.

Gade, M. and W. Alpers (1999): Using ERS-2 SAR images for routine observation of marine pollution in European coastal waters, *Sci. Total Environ.*, 237-238, 441-448.

Glazkova, I.A. and M.A. Stefanofskiy (2004): Development of program of remote sensing of the Earth at Khrunichev ГКНПЦ . 2004. *Second Open All-Russian Conference "Actual problems of Space remote sensing of Earth"*, Moscow, 16-18 November, 2004, 126-133 (in Russian).

Golik, A.V., V.K. Fischenko, V.A. Dubina and L.M. Mitnik (2004): Integration of satellite and ground-truth data for the Northwestern Pacific Ocean in corporative oceanographic GIS of FEB RAS. *Investigation of the Earth from Space,* in press (in Russian).

Golik, A.V., V.K. Fischenko, V.A. Dubina and L.M. Mitnik (2004): Usage of Internet-based GIS of POI FEB RAS in satellite oceanography. *Proc. 25th Asian Conference on Remote Sensing,* Thailand, 22-26 November 2004.

Ivanov, A.Yu. (2000): Oil pollution of the sea on Kosmos-1870 and Almaz-1 radar imagery, *Earth Observation & Remote Sensing,* 15, No. 6, 949-966.

Ivanov, A.Yu., K.Òs. Litovchenko and S.A. Ermakov (1998): Oil spill detection in the sea using Almaz-1 SAR. *J. Advanced Marine Science Technology Society,* 4, No. 2, 281-288.

Ivanov, A., M.-X. He and M.-Q. Fang (2002): Oil spill detection with the RADARSAT SAR in the waters of the Yellow and East China Sea: A case study. *Proc. 23rd Asian Conference on Remote Sensing,* 25-29 November 2002, Kathmandu, Nepal (http://www-gisdevelopment.net/aars/2002/sar/011.pdf

Ivanov, A.Yu., M.-X. He and M.-Q. Fang (2004): An experience of using ERS-1/2, Envisat and Radarsat images for oil spills mapping in the waters of the Caspian, Yellow and East China Sea. *Envisat & ERS ESA Symposium* (Salzburg, Austria, 6-10 September 2004).

Kalmykov, A.I. (1996): Real Aperture Radar (RAR) Imaging from Space. *Radio Science Bulletin,* N 276, 13-22.

Karlin, L.N. (ed). (1999): *Atlas of Synthetic Aperture Radar Images of the Ocean Acquired by ALMAZ-1 Satellite.* GEOS Publishing House, Moscow, 119 pp.

Kopelevich, O.V. (2001): The current low-parametric models of seawater optical properties. *Proc. Intern. Conference "Current Problems in Optics of Natural Waters" (0NW'2001)*, I. Levin and G. Gilbert (eds.), St. Petersburg, 2001, 18-23.

Kopelevich, O.V., V.I. Burenkov, S.V. Sheberstov, S.V.Vazyulya, E.A.Lukianova and M.A. Evdoshenko (2003): Mean monthly distributions of bio-optical characteristics in the Barents, White, Caspian, Black and Japan Seas from the data of the SeaWiFS satellite ocean color scanner. *Shirshov Institute of Oceanology. Russian Academy of Sciences*, http://manta.sio.rssi.ru/

Kostianoy, A.G., S.A. Lebedev, K.Ts. Litovchenko, S.V. Stanichny and O.E. Pichuzhkina (2004): Satellite remote sensing of oil spill pollution in the southeastern Baltic Sea. *Gayana*, vol. 68, N 2, 327-332.

Kostianoy, A.G., A.I. Ginzburg, S.A. Lebedev, M. Frankignoulle and B. Delille (2004): Oceanic front in the Southern Indian Ocean as inferred from the NOAA SST, TOPEX/Poseidon and ERS-2 altimeter data. *Gayana*, vol. 68, N 2, 333-339.

Kotlyakov, V.M. and L.V. Desinov (2004): Ecological monitoring from Russian segment of International Space Station. *Second Open All-Russian Conference "Actual problems of Space remote sensing of Earth"*, Moscow, 16-18 November, 2004, 24 (in Russian).

Lavrova O.Yu, and T.Yu. Bocharova (2003): Problems of oil pollution detection in the Black Sea coastal zone with using radar techniques. *All-Russian Conference "Actual problems of Space remote sensing of Earth"*, Moscow, 10-12 November, 2003, 38 (in Russian).

Lavrova O.Yu, M.I. Mityagina, A.G. Kostyanoy and K.Ts. Litovchenko (2004): Radar satellite monitoring of oil pollution in the coastal zone of the Russian seas. *Second Open All-Russian Conference "Actual problems of Space remote sensing of Earth"*, Moscow, 16-18 November, 2004, 146-147 (in Russian).

Lee, Z., K.L. Carder, C.D. Mobley, R.G. Steward and J.S. Patch (1998): Hyperspectral remote sensing for shallow waters. A semianalytical model, *Appl. Opt.*, vol. 37, no. 27, 6329-6338.

Lichtenegger, J., Using ERS-1 SAR images for oil spill surveillance (1994): http://esapub.esa.int/eoq/eoq44/lichten.htm

Lichtenegger, J., G. Calabresi and A. Petrocchi (2000): A Near-Real Time Oil Slick Monitoring Demonstrator for the Mediterranean. *IAPRS*, Vol. XXXXIII, Amsterdam, 8 pp.

Litovkin, D. (2004): The rocket-carrier "Cyclone-3" did not meet the challenge. "*Izvestiya*", 27 December 2004. http://www.izvestia.ru/armia2/article922373

Lupyan, E.A., A.A. Mazurov, R.R. Nazirov, A.A. Proshin and E.V. Flitman (2004): Technology of automatic information system construction for collection, processing and archiving of satellite data used for solving of scientific and applied tasks. In: *Actual problems of Space remote sensing of Earth.* E.A. Lupyan and O.Yu. Lavrova (eds.) Moscow, Poligraph service Publishing House, 81-89 (in Russian).

Mitnik, L.M. (2003): Microwave sensing of the ocean-atmosphere system: current state and outlooks. *Vestnik DVO*. № 3, 47-55 (in Russian).

Mitnik, L.M. (2004): Validation of AMSR-based algorithms and microwave study of marine weather systems. Paper presented at *ADEOS-II PI Workshop*, 8-10 December 2004, Nagahama, Japan, http://sharaku.eorc.jaxa.jp/ADEOS2/ws_nagahama/

Mitnik, L. and V. Dubina (2003): Features of surface circulation in the Aniva Bay and surrounding waters as seen by ERS synthetic aperture radar. *Proc. 18th Intern. Symposium on the Okhotsk Sea and Sea Ice*. Mombetsu, Hokkaido, Japan, 22-27 February 2003, 257-264.

Mitnik L.M., V.A. Dubina and G.V. Shevchenko (2004a): ERS SAR and Envisat ASAR observations of oceanic dynamic phenomena in the southwestern Okhotsk Sea. *Envisat & ERS ESA Symposium* (Salzburg, Austria, 6-10 September 2004), 10 pp.

Mitnik, L.M., M.L. Mitnik and V.A. Dubina (2004c): Marine weather systems: Study with ADEOS-II AMSR, Aqua AMSR-E and Envisat ASAR. *Gayana*, V. 68, No. 2, 389-395.

Mitnik, L.M. and M.L. Mitnik (2003): Retrieval of atmospheric and ocean surface parameters from ADEOS-II AMSR data: comparison of errors of global and regional algorithms. *Radio Sciences*. V. 38, No. 4, 8065, doi: 10.1029/2002RS002659.

Mitnik, L.M., G.V. Shevchenko, V.A. Dubina and Yu.A. Sophienko (2004b): Okhotsk Sea waters around Cape Krilion: Satellite and mooring station observations. *PICES Scientific Report*. No. 26. Proc. Third Workshop on the Okhotsk Sea and Adjacent Areas, S. McKinnell (ed), 98-101.

Mitnik L.M., H-J. Yoon, V.A. Dubina, Y-S. Kim and S.-W. Kim (2003b): ERS SAR observations of the Korean coastal waters. *The 24th Asian Conference on Remote Sensing & 2003 International Symposium on Remote Sensing*. Busan, Korea, 3-7 November 2003, Vol. 1, 228-230.

Mitnik, L.M. and S.V. Victorov (eds.) (1990: *Radar Sensing of the Earth's Surface from Space (Radiolokatsiya poverkhnosti Zemli iz kosmosa)*. Hydrometeoizdat Publishing House, Leningrad, 200 pp. (in Russian)

Mityagina, M.I., A. Churumov and O. Lavrova (2004): Problems in Detecting Oil Pollution in Black Sea Coastal Zone by Satellite Radar Means. *Envisat & ERS ESA Symposium* (Salzburg, Austria, 6-10 September 2004).

Nelepo, B.A., Y.V. Terekhin, V.K. Kosnirev and B.E. Khmirov (1983): *Satellite Hydrophysics (Sputnikovaya Hydrophysica)*. Nauka Publishing House, Moscow, 254 pp. (in Russian).

Ohshima K.I. and M. Wakatsuchi (1990): A numerical study of barotropic instability associated with the Soya Warm Current in the Sea of Okhotsk. *J. Phys. Oceanogr.*, vol. 20, 570-584.

Park, Y.H. and L. Gamberoni (1995): Large-scale circulation and its variability in the South Indian Ocean from TOPEX/POSEIDON altimetry. *J. Geophys. Res.*, vol. 100, No. C12, 31447-31462.

Pavlakis, P., D. Tarchi, and A. J. Sieber (2001): On the monitoring of illicit vessel discharges using spaceborn SAR remote sensing - a reconnaissance study in the Mediterranean Sea. *Ann. Telecommun*, 56, No. 11-12, 700-718.

Protsenko, I.G., V.Yu Reznikov, M.V. Andreev, A.V. Babyuk et al. (2004): Technological structure of fishery monitoring system in Far Eastern region. *Second Open All-Russian Conference "Actual problems of Space remote sensing of Earth"*, Moscow, 16-18 November, 2004, 72 (in Russian).

Shin, C.-W., Byun S.-K., C. Kim and Y.H. Seung (2000): Warm core in the East Korean Bay in winter. In: *Oceanography of the Japan Sea*. Proc. CREAMS'2000 Intern. Symposium. M.A. Danchenkov (ed.). Vladivostok, Dalnauka, 41-46.

Suh, Y.S., S.D. Hahn, Y.Q. Kang, and B.G. Mitchell (1998): Study of a recurring anticyclonic eddy off the northeast Korean coast using satellite ocean color and sea surface temperature imagery. *J. Advanced Marine Science Technology Society*, vol. 4, 275-280.

Solberg, A. H. S., G. Storvik, R. Solberg and E. Volden (1999): Automatic detection of oil spills in ERS SAR images. *IEEE Trans. Geosci. Remote Sens.*, 37, No. 4, 1916-1924.

Solberg, A.H.S., S.T. Dokken and R. Solberg (2003): Automatic detection of oil spills in Envisat, Radarsat and ERS SAR images. *Proc. IGARSS 2003*, Vol. IV, 2747-2749.

Solberg, A.H.S. (2004): paper presented at *Envisat & ERS ESA Symposium* (Salzburg, Austria, 6-10 September 2004).

Trenina, I.S. (2004): Space monitoring of ice cover for operational mapping and long-term investigations. In: *Actual problems of Space remote sensing of Earth.* E.A. Lupyan and O.Yu. Lavrova (eds.), Moscow, Poligraph service Publishing House, 303-313 (in Russian).

Wilson, W.S., J.-L. Fellous, H. Kawamura and L. Mitnik (2006): A History of Oceanography from Space. In: *Manual of Remote Sensing*, Vol. 6, Chapter 1. John Wiley, in press.

Zabolotskikh, E.V., L.M. Mitnik, L.P. Bobylev and O.M. Johannessen (2000): Development and validation of algorithms for sea surface wind speed retrieval from SSM/I data with using neural networks and physical constrains. *Earth Observation and Remote Sensing*, vol. 9, 43-55 (in Russian and translated into English).

Zabolotskikh, E.V., L.M. Mitnik, L.P. Bobylev and O.M. Johannessen (2004): Neural network algorithms for retrieval of the ocean-atmosphere system parameters from microwave satellite sensing data. In: *Actual problems of Space remote sensing of Earth.* E.A. Lupyan and O.Yu. Lavrova (eds.) Moscow, Poligraph service Publishing House, 447-458 (in Russian).

LIST OF ACRONYMS

ADEOS	Advanced Earth Observing Satellite
ALOS	Advanced Land Observing Satellite
AMSR	Advanced Microwave Scanning Radiometer
AMSR-E	Advanced Microwave Scanning Radiometer for EOS
ASAR	Advanced synthetic aperture Radar
AVHRR	Advanced Very High Resolution Radiometers
CEARAC	Coastal Environmental Assessment Regional Activity Center
Chl *a*	chlorophyll *a*
EKWC	East Korean Warm Current
ENVISAT	Environment Satellite
ERS-1/2	European Remote Sensing Satellites-1/2
ESA	European Space Agency
ESIMO	
FEB	Far Eastern Branch
FSP	Federal Space Program
GCMD	Global Change Master Directory
GIS	Geoinformation System
GMS	Geostationary Meteorological Satellite
GOMS	Geostationary Meteorological Satellite System
GOOS	The Global Ocean Observing System
GPS	Global Position System
HABs	Harmful Algal Blooms
HRPT	High Resolution Picture Transmission
IACP	Institute of Automatic and Control Processes
IKI	Space Research Institute
IMB	Institute of Marine Biology
IWs	Internal Waves
JAXA	Japan Aerospace Exploration Agency
JMA	Japan Meteorological Agency
MIVZA	Microwave Scanning Radiometer
MODIS	Moderate Resolution Imaging Spectrometer
MTVZA-OK	Scanning Microwave Radiometer
MSU	Multiband Scanning Unit
MVISR	Multi-channel Visible and IR Scan Radiometer
NEAR-GOOS	North-East Asian Regional GOOS
NOAA	National Oceanic and Atmospheric Administration
NOWPAP	Northwest Pacific Action Plan
NPEC	Northwest Pacific Region Environmental Cooperation Center
PICES	the North Pacific Marine Science Organization
POI	Pacific Oceanological Institute
QL	Quick Look
QuikSCAT	Quick Scatterometer
RAR	Real Aperture Radar
RAS	Russian Academy of Sciences
RS	Remote Sensing
SAR	Synthetic Aperture Radar
SeaWiFS	Sea-viewing Wide Field-of-view Sensor
SLA	Sea Level Anomaly
SRC	Scientific Research Center
SST	Sea Surface Temperature
SWC	Soya Warm Current
TWC	Tsushima Warm Current
VIRS	Visible and Infrared Scanner

UNEP	United Nations Environment Programme
WESTPAC	Western Pacific
WSC	West Sakhalin Current